

5-2023

## Formation Control of Multiple Quadrotors

Miguel Alejandro Garcia  
*The University of Texas Rio Grande Valley*

Follow this and additional works at: <https://scholarworks.utrgv.edu/etd>



Part of the [Electrical and Computer Engineering Commons](#)

---

### Recommended Citation

Garcia, Miguel Alejandro, "Formation Control of Multiple Quadrotors" (2023). *Theses and Dissertations*. 1216.

<https://scholarworks.utrgv.edu/etd/1216>

This Thesis is brought to you for free and open access by ScholarWorks @ UTRGV. It has been accepted for inclusion in Theses and Dissertations by an authorized administrator of ScholarWorks @ UTRGV. For more information, please contact [justin.white@utrgv.edu](mailto:justin.white@utrgv.edu), [william.flores01@utrgv.edu](mailto:william.flores01@utrgv.edu).

FORMATION CONTROL OF MULTIPLE QUADROTORS

A Thesis

by

MIGUEL ALEJANDRO GARCIA

Submitted in Partial Fulfillment of the

Requirements for the Degree of

MASTER OF SCIENCE IN ENGINEERING

Major Subject: Electrical Engineering

The University of Texas Rio Grande Valley

May 2023



# FORMATION CONTROL OF MULTIPLE QUADROTORS

A Thesis  
by  
MIGUEL ALEJANDRO GARCIA

## COMMITTEE MEMBERS

Dr. Wenjie Dong  
Chair of Committee

Dr. Weidong Kuang  
Committee Member

Dr. Alexander Domijan  
Committee Member

May 2023



Copyright 2023 Miguel Alejandro Garcia

All Rights Reserved



## ABSTRACT

Garcia, Miguel A., Formation Control of Multiple Quadrotors. Master of Science in Engineering (MSE), May, 2023, 72 pp., 42 figures, references, 60 titles.

This thesis studies formation control of multiple quadrotors under different conditions. Two controller design approaches are proposed. In the first approach, it is assumed that the dynamics of each quadrotor is unknown and there is disturbance. With the aid of distributed estimation and the universal approximation property of neural networks, distributed tracking controllers are proposed. Simulation shows the effectiveness of the proposed controllers. In the second approach, it is assumed that the inertia parameters are unknown. With the aid of distributed estimation, online data estimation, and optimal control theory, distributed sub-optimal tracking controllers are proposed. Simulation results show the effectiveness of the proposed controllers.



## DEDICATION

I would like to dedicate this thesis/dissertation to all my friends, family, and educators that have always pushed me to be the best that I can be. Thank you for showing me the sky is the limit.



## ACKNOWLEDGMENTS

Dr. Wenjie Dong cooperation and dedication have been challenging yet inspirational and rewarding. Through his knowledge and experience, I was able to propose some impactful work that I see being use of in practical applications. I would also like to thank Dr. Weidong Kuang and Dr. Alexander Domijan for always being available to listen to my questions throughout my time at UTRGV. With this committee, and their vast knowledge of different areas of Electrical Engineering, I was able to challenge myself during this pursuit of the Master's degree.

Lastly, this work couldn't not have been done without the support of the NSF grant ECCS2037649...



## TABLE OF CONTENTS

	Page
ABSTRACT .....	iii
DEDICATION .....	iv
ACKNOWLEDGEMENTS .....	v
TABLE OF CONTENTS.....	vi
LIST OF FIGURES.....	viii
CHAPTER I. INTRODUCTION.....	1
1.1 Topics in the Thesis.....	.6
1.2 Thesis Contribution .....	.6
CHAPTER II. DISTRIBUTED TRACKING CONTROL OF MULTIPLE QUADROTORS WITH THE AID OF NEURAL NETWORKS .....	.8
2.1 Problem Statement and Preliminaries.....	8
2.1.1 Problem Statement.....	.8
2.1.2 Neural Networks.....	13
2.2 Controller Design.....	16
2.2.1 Distributed Estimator Design.....	16
2.2.2 Tracking Controller Design.....	17
2.3 Simulation Results.....	27
2.4 Conclusion.....	33
CHAPTER III. DISTRIBUTED TRACKING CONTROL OF MULTIPLE QUADROTORS WITH THE AID OF OPTIMAL CONTROL THEORY .....	34
3.1 Introduction.....	34

3.2 Problem Statement and Preliminaries. . . . .	34
3.2.1 Problem Statement. . . . .	34
3.3 Controller Design . . . . .	39
3.3.1 Distributed Estimator Design. . . . .	39
3.3.2 Parameter Estimation. . . . .	40
3.3.3 Optimal Tracking Controller Design. . . . .	42
3.4 Simulation Results. . . . .	50
3.5 Conclusion. . . . .	57
CHAPTER IV. FUTURE WORK. . . . .	63
REFERENCES. . . . .	64
BIOGRAPHICAL SKETCH. . . . .	72

## LIST OF FIGURES

	Page
Figure 2.1 Biology of a neuron . . . . .	13
Figure 2.2 Structure of neural networks. . . . .	13
Figure 2.3 Connection of a node. . . . .	14
Figure 2.4 Neural networks [1] . . . . .	14
Figure 2.5 Function approximation of NNs. . . . .	15
Figure 2.6 Configuration of a quadrotor. . . . .	26
Figure 2.7 Communication graph between quadrotors. . . . .	28
Figure 2.8 Desired formation. . . . .	28
Figure 2.9 Estimate errors $p_0 - \hat{p}_j$ for $1 \leq j \leq 3$ . . . . .	29
Figure 2.10 Estimate errors $v_0 - \hat{v}_j$ for $1 \leq j \leq 3$ . . . . .	30
Figure 2.11 Estimate errors $\psi_0 - \hat{\psi}_j$ for $1 \leq j \leq 3$ . . . . .	30
Figure 2.12 Tracking errors $p_j - h_j - (p_0 - h_0)$ for $1 \leq j \leq 3$ . . . . .	31
Figure 2.13 Tracking errors $s_j$ for $1 \leq j \leq 3$ . . . . .	31
Figure 2.14 Tracking errors $\tilde{q}_j$ for $1 \leq j \leq 3$ . . . . .	32
Figure 2.15 Tracking errors $\tilde{\omega}_j$ for $1 \leq j \leq 3$ . . . . .	32
Figure 3.1 Configuration of a quadrotor . . . . .	50
Figure 3.2 Communication graph between quadrotors . . . . .	51
Figure 3.3 Desired formation . . . . .	52
Figure 3.4 Estimation error $p_0 - \hat{p}_1$ . . . . .	52
Figure 3.5 Estimation error $v_0 - \hat{v}_1$ . . . . .	52
Figure 3.6 Estimation error $b_{2,0} - \hat{r}_1$ . . . . .	53

Figure 3.7	Estimation error $p_0 - \hat{p}_2$ . . . . .	53
Figure 3.8	Estimation error $v_0 - \hat{v}_2$ . . . . .	54
Figure 3.9	Estimation error $b_{2,0} - \hat{r}_2$ . . . . .	54
Figure 3.10	Estimation error $p_0 - \hat{p}_3$ . . . . .	55
Figure 3.11	Estimation error $v_0 - \hat{v}_3$ . . . . .	55
Figure 3.12	Estimation error $b_{2,0} - \hat{r}_3$ . . . . .	55
Figure 3.13	Time response of the estimate of $m$ . . . . .	56
Figure 3.14	Time response of the estimate of $J$ . . . . .	57
Figure 3.15	The tracking error $p_1 - h_1 - (p_0 - h_0)$ . . . . .	58
Figure 3.16	The tracking error $p_2 - h_2 - (p_0 - h_0)$ . . . . .	58
Figure 3.17	The tracking error $p_3 - h_3 - (p_0 - h_0)$ . . . . .	58
Figure 3.18	The tracking error $v_1 - v_0$ . . . . .	59
Figure 3.19	The tracking error $v_2 - v_0$ . . . . .	59
Figure 3.20	The tracking error $v_3 - v_0$ . . . . .	59
Figure 3.21	The tracking error $\tilde{q}^1$ . . . . .	60
Figure 3.22	The tracking error $\tilde{q}^2$ . . . . .	60
Figure 3.23	The tracking error $\tilde{q}^3$ . . . . .	60
Figure 3.24	The tracking error $\tilde{\omega}^1$ . . . . .	61
Figure 3.25	The tracking error $\tilde{\omega}^2$ . . . . .	61
Figure 3.26	The tracking error $\tilde{\omega}^3$ . . . . .	62

## CHAPTER I

### INTRODUCTION

There has been an active case of research about control of quadcopters due to its potential applications in both civil and military uses such as surveillance, search and rescue missions and observation/monitoring objectives. Quadcopters have three degrees of freedom (DOF) in the translational motion allowing the vehicle to travel in the x, y, and z-axis in addition to the three DOF in the rotational motion that allow them to fly in any desired orientation. Essentially quadcopters can fly in any position with any desired orientation. In addition, quadcopters can operate in cluttered environments and have the benefit to hover for long period of time. On the other hand, a quadcopter generally has four inputs which makes the nature of the system an underactuated system which in return makes the control of the quadcopter a challenging dilemma.

The dynamics of a quadcopter can be considered as a cascaded system which includes a position control subsystem and an orientation control subsystem. Taking into consideration aid of the featured cascade structure, a controller can be designed in a couple of steps. The first step would be to design a virtual controller such that the position of the quadcopter would converge to its designed position. The problem in the first step would be called the position tracking problem. The second step allows a controller to be designed with the aid of the virtual controller from the first step such that the position and orientation of the quadcopter converge to its desired position and orientation, respectively. The problem in this step is called the attitude tracking problem. Different controllers were proposed with the aid of the backstepping technique in [2-6]

based on the cascade structure. In addition, different techniques applied allowed there to be the designing of controllers. Feedback linearization being applied helped design tracking controllers in [7,8]. In [9,10], controllers were proposed with the aid of model predictive control. [11,12] designed tracking controllers that were proposed using the sliding mode technique. Robust control techniques are effective tools dealing with non-parametric uncertainty. Different robust controllers have been proposed with the aid of different robust techniques. Sliding mode control techniques were applied to estimate disturbance which resulted in the sliding mode based tracking controller in [12]. Sliding mode techniques were applied to compensate for un-modeled dynamics and adaptive robust tracking controllers that were proposed in [13,14].

The parameters of attitude of quadcopters in attitude tracking control can be represented by Euler angles, modified Rodrigues parameters (MRPs), or the unit quaternion. Controllers designed on Euler angles and MRPs have singularities which reduces the ability to achieve large angular maneuvers. In order to fix the issue stated, the unit quaternion is used to help define the attitude of a quadcopter and controllers are designed with the aid of the unit quaternion. Since quaternions have ambiguities in representing an attitude (two quaternions represent an attitude), the controllers design based on quaternions are sensitive to small measurement noises and may exhibit unwinding behavior where the UAV makes an unnecessary full rotation [15-17]. Hybrid controllers were proposed in [2,18] to overcome the unwinding dilemma. In the two-step controller design stated above a crucial assumption is made to obtain the well-defined controller, which is that the total thrust is nonzero at any given time. To satisfy this assumption many papers assume that the reference total thrust is bounded away from zero and the initial errors between the state of the system and the desired value of the state of the system are sufficiently small. Therefore, the controllers proposed in these papers are locally well-defined.

Well-defined controllers for large attraction region with aid of saturation control in [19,20] is proposed to aid the issue. The tracking control of a quadcopter is not taken into account for when the mass and the moment of a quadcopter are unknown.

Uncertainty is always in practice when discussing the control of quadcopters. Generally, there are two types of uncertainty. The unknown information of the mass and the inertia moment of quadcopter is labeled as parametric uncertainty. The other type of uncertainty is the non-parametric uncertainty which involves un-modeled dynamics and disturbances. Different adaptive methods have been applied to design adaptive controllers when dealing with parametric uncertainty. Immersion and invariance techniques were applied to design adaptive controllers in [21,22]. In [23], adaptive backstepping technique was applied and an adaptive tracking controller was proposed. Adaptive backstepping technique and command-filter compensation were applied in [24] and adaptive tracking controllers were proposed without computation of derivatives of signals.

The need for sensors being equipped for measuring the linear and angular velocity is crucial because they become available for feedback control. Because of this attitude tracking control of quadcopters without velocity measurements was extensively studied. If angular velocity is not available for feedback control, the output based attitude tracking controllers were extensively studied. There are generally two types of output tracking controllers. Observer-based controllers are designed based on the observer-based approach and observer-free controllers which are designed by other approaches instead of the observer-based approach [18,27]. The observer-based approach basically dictates that an observer is designed first and the tracking controller is designed with the aid of the observer and other properties of the system [25,26]. For position and attitude tracking control of quadcopters, if the linear velocity is not available then

an output controller is proposed using the aid of a singular perturbation listed in [28]. [29] proposes an output controller with the aid of a nonlinear observer design. There are few research results except for the paper [30] that discuss if both the linear and angular velocities are non-available for feedback control of the quadcopters.

More complex tasks have a better application for multiple quadcopters to perform the objective. Formation flying of multiple quadcopters has been on the latest research due to its wide applications of military and civilian use such as surveillance, search/rescue tasks, area exploration and many other needs. The limitless capacity of vertical taking-off and landing (VTOL) cues makes the quadcopter superior to other UAVs. The formation of multiple quadcopters can perform more complex tasks and provide better performance in comparison to the performance of a single quadcopter, however, the underactuated nature of a single quadcopter makes the cooperative control of multiple quadcopters even more challenging.

One of the goals of formation control of multiple quadcopters is to coordinate a group of quadcopters to achieve a desired spatial geometric pattern. Several classical approaches have been proposed for multi-agent systems such as the behavioral approach, the virtual structure approach, leader-follower approach, and the graph theoretical approach. In the leader-follower approach [31,32], some agents are designed to be leaders and others are followers. The leader tracks the predefined trajectories while the followers track the state of their neighboring vehicles according to a given scheme. The behavioral approach [33-35] discusses the control action for each agent by being defined as a weight average of the control corresponding to each desired behavior of the agent. In the virtual structure approach [36-38], the entire formation is treated as a single rigid body. The structure in [36-38] moves along a desired trajectory and with a desired attitude. In the graph theoretical approach [39-42] the idea of each agent is considered

as a node and the communication between the agents is presented in a communication graph which allows the control law to be designed by the difference of neighboring information.

The formation control of multiple unmanned aerial vehicles (UAVs) has been studied extensively. In [43,44] the dynamics of each vehicle are represented by a simplified linear system and the formation control is studied based on multiple linear systems. [45-47] studies translational and rotational motions with linear and simplified models. Formation control of multiple UAVs has been studied in [48-51] based on a six DOF model, noting that UAVs are a multiple input/output system with high nonlinear and coupled dynamics. In [49,50] the formation control of multiple UAVs as studied with disturbances and robust distributed control laws were proposed using the same six DOF model. [51] studies non-smooth backstepping design on the distributed formation control of multiple UAVs and consensus techniques for the 6 DOF model.

The formation controllers in the above literatures secure the states of a UAV asymptotically converges to a desired formation as time continues to infinity. Finite-time distributed controllers are preferred in practical applications because they guarantee the states of a UAV converge to a desired formation within a finite time and reduce the disturbance rejection performance due to the closed loop systems. [52] studies the non-parametric uncertainties in formation control of multiple UAVs which resulted in the proposal of finite-time controllers with the aid of finite-time distributed observers. The aid of homogenous systems was used in [46] to propose finite-time distributed controllers based on the linearized models without uncertainty. The Euler angles define the attitudes of the UAVs in [46,52]. To make the attitude control laws nonsingular, the Euler angles are given a limited interval.

## 1.1 Topics in the Thesis

Motivated by the research work mentioned above and the work in [53–55], in this thesis we will study the formation control of multiple quadrotors with a leader by different techniques.

In the first problem considered in this thesis, we study the formation control of multiple quadrotors with unknown dynamics. In this problem, it is assumed that the information of the leader system is not available to all follower systems and it is also assumed that the dynamics of each system is not well-known. In order to solve the formation problem, a multiple-step approach is proposed with the aid of distributed estimation, neural networks, and the backstepping techniques. Distributed controllers are proposed based on this approach.

In the second problem considered in this thesis, we study the optimized formation control of multiple quadrotors with unknown dynamics. In this problem, it is assumed that the information of the leader system is not available to all follower systems and it is also assumed that the inertia parameters of each system is not well-known. In the controller design, it is required to propose distributed controllers such that some performance to be minimized. To this end, a multiple-step approach is proposed with the aid of distributed estimation, on-line parameter estimation, optimal control, and the backstepping techniques. Distributed controllers are proposed with the aid of this approach.

## 1.2 Thesis Contribution

The contributions of our work are as follows.

- A new multi-step networked-based approach is proposed for formation control of multiple quadrotors. In this approach, the unknown dynamics and uncertain environment are approximated by neural networks. Due to the universal approximation property of neural

networks, the proposed distributed controllers can learn unknown dynamics and environment very well and make the performance of the whole system better.

- A new multi-step optimized controller design approach is proposed for formation control of multiple quadrotors. In this approach, the unknown parameters are estimated based on on-line data and distributed controllers are proposed with the aid of optimal control theory. So, the proposed controllers are sub-optimal in some sense of performance, which is better than the controllers proposed without performance requirements.

The proposed controller design approach can be applied to design formation controller for other types of unmanned aerial vehicle.

## CHAPTER II

### DISTRIBUTED TRACKING CONTROL OF MULTIPLE QUADROTORS WITH THE AID OF NEURAL NETWORKS

Although there are many results on formation control of multiple quadcopters, how to improve the control performance is still challenging in the presence of uncertainty and coupling among neighboring quadrotors. Motivated by the research work in [53–55], in this chapter we study the formation control of multiple quadrotors with parametric and non-parametric uncertainties and propose new distributed control laws with the aid of neural networks such that the formation errors converge to zero and the attitude of each quadrotor converges to a desired attitude. In order to solve the formation control problem, a multi-step approach is proposed and distributed control laws are proposed.

#### 2.1 Problem Statement and Preliminaries

##### 2.1.1 Problem Statement

Consider  $m$  quadrotors. Under some assumptions, the kinematics and dynamics of  $j$ -th quadrotor are defined by

$$\dot{p}_j = v_j \quad (2.1)$$

$$\dot{v}_j = -g e_3 + \frac{1}{m_j} f_j R_j e_3 + d_{1j} \quad (2.2)$$

$$\dot{R}_j = R S(\omega_j) \quad (2.3)$$

$$J_j \dot{\omega}_j = S(J_j \omega_j) \omega_j + \tau_j + d_{2j} \quad (2.4)$$

where  $p_j$  and  $v_j$  are the position and the velocity of the mass center in the inertia frame, respectively,  $g$  is the gravitational acceleration,  $e_3 = [0, 0, 1]^\top$ ,  $f_j \in \mathbb{R}$  is the total thrust,  $R_j = [b_{1j}, b_{2j}, b_{3j}]$  is the rotation matrix of the body frame with respect to the inertia frame,  $\omega_j$  is the angular velocity of the quadrotor in its body frame,  $J_j$  is the inertia moment of the quadrotor,  $d_{1j}$  and  $d_{2j}$  denote non-parametric uncertainty and disturbance,  $S(\zeta)$  for  $\zeta = [\zeta_1, \zeta_2, \zeta_3]^\top$  is a skew-symmetric matrix defined by

$$S(\xi) = \begin{bmatrix} 0 & -\xi_3 & \xi_2 \\ \xi_3 & 0 & -\xi_1 \\ -\xi_2 & \xi_1 & 0 \end{bmatrix}$$

and  $\tau_j = [\tau_{1j}, \tau_{2j}, \tau_{3j}]^\top$  is the torque input of the system. Let  $\Theta_j = [\varphi_j, \theta_j, \psi_j]^\top$  be the Euler angles of frame of the  $j$ -th vehicle, the attitude of the vehicle can be defined by  $\Theta_j$ . The relation between the Euler angles and the rotation matrix is

$$R_j = \begin{bmatrix} c\theta_j c\varphi_j & s\theta_j c\varphi_j s\phi_j - s\varphi_j c\phi_j & s\theta_j c\varphi_j c\phi_j + s\varphi_j s\phi_j \\ c\theta_j s\varphi_j & s\theta_j s\varphi_j s\phi_j + c\varphi_j c\phi_j & s\theta_j s\varphi_j c\phi_j - c\varphi_j s\phi_j \\ -s\theta_j & c\theta_j s\phi_j & c\theta_j c\phi_j \end{bmatrix} \quad (2.5)$$

where  $c\theta_j$  denotes  $\cos\theta_j$  and  $s\theta_j$  denotes  $\sin\theta_j$ . To make the mapping from the attitude to the Euler angles one-to-one, we restrict the Euler angles to the following regions:

$$\phi_j \in \left(-\frac{\pi}{2}, \frac{\pi}{2}\right), \theta_j \in \left(-\frac{\pi}{2}, \frac{\pi}{2}\right), \varphi_j \in (-\pi, \pi). \quad (2.6)$$

By simple algebraic calculation, (2.3) can be written as

$$\dot{\Theta}_j = W(\Theta_j) \omega_j \quad (2.7)$$

where

$$W(\theta_j) = \frac{1}{\cos\theta_j} \begin{bmatrix} \cos\theta_j & \sin\phi_j \sin\theta_j & \cos\phi_j \sin\theta_j \\ 0 & \cos\phi_j \cos\theta_j & -\sin\phi_j \cos\theta_j \\ 0 & \sin\phi_j & \cos\phi_j \end{bmatrix}$$

and  $\det(W(\theta_j)) = \frac{1}{\cos\theta_j}$ .  $W$  is nonsingular if  $\theta_j \neq \frac{(2k-1)\pi}{2}$  for any integer  $k$ .

For multiple quadrotors, there are information flows between them with the aid of sensors or wireless communication. Consider each quadrotor as a node. The communication between quadrotors is defined by a directed graph  $G = \{A, E\}$  where  $A$  is the node set and  $E$  is the edge set. If there is an edge  $e_{ij}$  in  $E$ , it means that the information of node  $i$  is available to node  $j$ . Node  $i$  is called a neighbor of node  $j$  if the information of node  $i$  is available to node  $j$ . All neighbors of node  $j$  form a node set which is called the neighbor set of node  $j$  and is denoted by  $N_j$ . A directed path from node  $i$  to node  $j$  is a sequence of sets of edges that connect node  $i$  to node  $j$  by following their directions. Node  $i$  is said to be reachable to node  $j$  if there exists a directed path from node  $i$  to node  $j$ . Node  $i$  is said globally reachable if node  $i$  is reachable for every other node in  $A$ .

In this chapter, we assume there are  $m$  follower quadrotors and one leader quadrotor. The leader quadrotor is operated by a human operator and does not receive any information from the follower quadrotors. Without loss of generality, the leader quadrotor is labeled as node 0. The follower quadrotors are labeled by 1, 2, ...,  $m$ . The communication between  $m + 1$  quadrotors is defined by an augmented directed graph  $G^a = \{A^a, E^a\}$  where  $A^a = A \cup \{0\}$  and  $E^a$  is a union of  $E$  and the edges from node 0 to the followers.

For  $m$  follower quadrotors and a leader quadrotor, a desired formation can be defined by  $(m+1)$  vectors  $h_j \in R^3$  which may be constant vectors or time-varying vectors. We say  $(m+1)$  quadrotors are in the desired formation if

$$p_i - p_j = h_i - h_j$$

for any  $0 \leq i, j \leq m$ . We say  $m + 1$  quadrotors come into the desired formation if

$$\lim_{t \rightarrow \infty} [(p_i - h_i) - (p_j - h_j)] = 0$$

for any  $0 \leq i, j \leq m$ .

In the dynamics (2.1)-(2.4), the parametric uncertainty (i.e.,  $m_j$  and  $J_j$ ) and non-parametric uncertainty (i.e.,  $d_{1j}$  and  $d_{2j}$ ) are called the *system uncertainty*. For each quadrotor, it is unknown whether the leader quadrotor is a neighbor or not. We say there is *information uncertainty* for each quadrotor.

In this chapter, we consider the following control problem.

**Formation flying with a leader:** For a leader quadrotor and  $m$  follower quadrotors, it is assumed that  $m_j$ ,  $J_j$ ,  $d_{1j}$ , and  $d_{2j}$  are unknown for  $1 \leq j \leq m$ . It is given the position and the orientation of a leader quadrotor and a desired formation defined by  $h_j$  for  $0 \leq j \leq m$ , the control problem is to design distributed state feedback controllers  $f_j$  and  $\tau_j$  using its own information and its neighbors' information such that

$$\lim_{t \rightarrow \infty} [(p_j - h_j) - (p_0 - h_0)] = 0 \quad (2.8)$$

$$\lim_{t \rightarrow \infty} [(\varphi_j(t) - \varphi_0(t))] = 0 \quad (2.9)$$

for  $1 \leq j \leq m$ .

In the defined problem, (2.8) means that the  $(m+1)$  quadrotors come into the desired formation and (2.9) means that the  $Y$  axes of the body frames of  $m + 1$  quadrotors are parallel as time goes to infinity.

In order to solve the defined problem, the following assumptions are made.

**Assumption 2.1.** *The mass  $m_j$  of quadrotor  $j$  is an unknown constant and  $\underline{m}_j \leq m_j \leq \overline{m}_j$  where  $\underline{m}_j$  and  $\overline{m}_j$  are known constants.*

**Assumption 2.2.** *The inertia matrix  $J_j$  of quadrotor  $j$  is an unknown constant matrix.*

**Assumption 2.3.**  *$d_{1j}$  and  $d_{2j}$  are continuous functions and are bounded.*

**Assumption 2.4.** *The communication graph  $G^a$  is a directed graph and the node 0 is globally reachable.*

**Assumption 2.5.**  *$p_0(t)$  is smooth  $\| \ddot{p}_0(t) \|$  and  $\| \ddot{p}_0 \|$  are bounded.*

**Assumption 2.6.**  *$\psi_0$  is smooth.  $\psi_0(t)$  is bounded.*

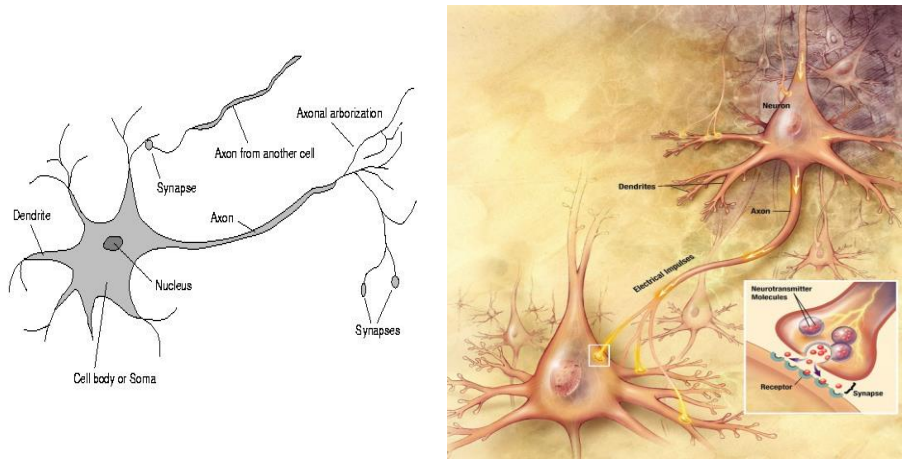


**Figure 2.1:** Biology of a neuron

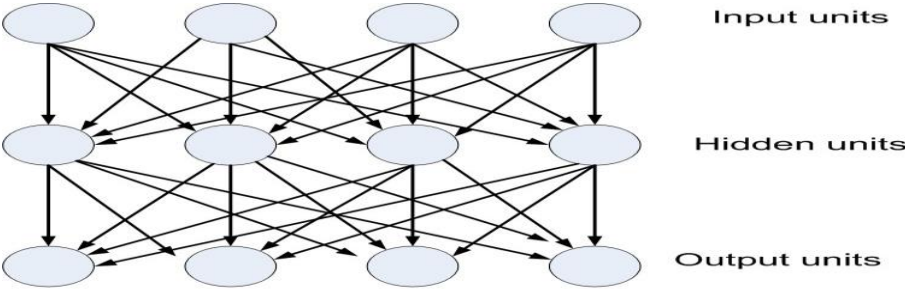


**Figure 2.2:** Structure of neural networks.

**2.1.2 Neural Networks**

We can learn things by our brains. In a brain, different areas have different functions. Some areas seem to have the same function in all humans (e.g., Broca’s region for motor speech); the overall layout is generally consistent. Some areas are more plastic, and vary in their function; also, the lower—level structure and function vary greatly. We don’t know how different functions are “assigned” or acquired.

Brain function occurs as the result of the firing of neurons. Neurons connect to each other through synapses (see Fig. 2.1), which propagate action potential (electrical impulses) by

releasing neurotransmitters. There are about  $10^{11}$  neurons and about  $10^{14}$  synapses in the human brain!

Neural networks are made up of nodes or units, connected by links (see Fig. 2.2). Each link

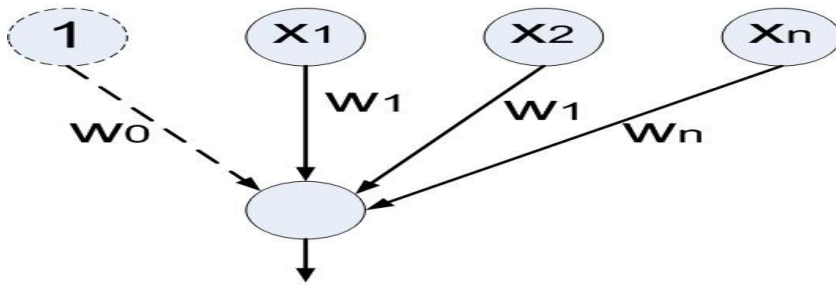


**Figure 2.3:** Connection of a node.

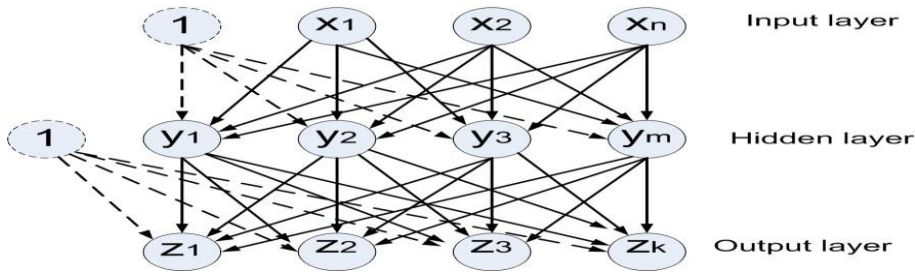


**Figure 2.4:** Neural networks [1].

has an associated weight and activation level. Each node has an input function (typically summing over weighted inputs), an activation function, and an output. For each node (Fig. 2.3), the output is

$$f = g(w^T x)$$

where  $x = [1, x_1, \dots, x_n]^T$  is the input vector,  $w = [w_0, w_1, \dots, w_n]^T$  is the weight vector,  $w_0$  is the bias,  $g(\cdot)$  is the activation function. A sigmoid (logistic) activation function is  $g(z) = \frac{1}{1+e^{-z}}$ . In a neural network (Fig. 2.4), the outputs the hidden layer are

$$y_i = g(W_i^T x), \quad 1 \leq i \leq m$$

where  $x = [1, x_1, \dots, x_n]^T$  is the input vector,  $w = [w_{0i}, w_{1i}, \dots, w_{ni}]^T$  is the weight vector,  $w_{0i}$  is the bias,  $g(\cdot)$  is the activation function.

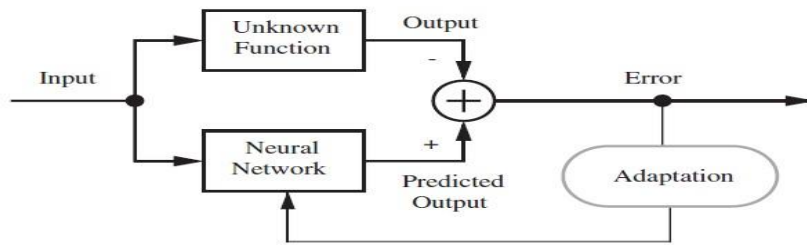


**Figure 2.5:** Function approximation of NNs

The outputs of the output layer are

$$z_i = g(\Theta_i^T y), \quad 1 \leq i \leq k$$

where  $y = [1, y_1, \dots, y_m]^T$ ,  $\Theta = [\theta_{0i}, \theta_{1i}, \dots, \theta_{mi}]^T$  is the weight vector,  $\theta_{0i}$  is the bias.

Neural networks can be applied to classification, pattern recognition, approximation, prediction, etc. Before its application, the neural network should be trained off-line or on-line.

Off-line Training is to find the weights with the aid of a cost function for each layer for given input data and the desired output data. There are many methods for off-line training. See some textbooks.

For control purpose, the neural network is used as an universal approximator. The neural network is trained on-line. The structure of function approximation with the aid of NNs is shown in Fig. 2.5 (see [1]). The ability of the approximation of NNs is as follows.

**Theorem:** (Universal approximation) Any continuous function  $f(x)$  defined in a compact set  $\Omega \in R^n$  can be approximated arbitrarily well by a neural network with at least 1 hidden layer with a finite number of weights.

## 2.2 Controller Design

In order to design distributed controllers, a two-step controller design procedure is proposed. In the first step, we design distributed estimators to estimate state of the leader vehicle using neighbors' information. In the second step, we design a adaptive tracking controller for each system such that the state of the vehicle asymptotically tracks the estimated state of the leader vehicle.

### 2.2.1 Distributed Estimator Design

In this section, we apply the results in [56] to design distributed estimators. Let  $(\hat{p}_j, \hat{v}_j, \hat{\psi}_j)$  be the estimate of the leader's state  $(p_0, v_0, \psi_0)$ . Based on the results in [56], the distributed estimators for vehicle  $j$  are proposed as follows.

$$\dot{\hat{p}}_j = - \sum_{i \in \mathcal{N}_j} a_{ji} (\hat{p}_j - \hat{p}_i) - \beta_p \text{sign} \left( \sum_{i \in \mathcal{N}_j} a_{ji} (\hat{p}_j - \hat{p}_i) \right) \quad (2.10)$$

$$\dot{\hat{v}}_j = - \sum_{i \in \mathcal{N}_j} a_{ji} (\hat{v}_j - \hat{v}_i) - \beta_v \text{sign} \left( \sum_{i \in \mathcal{N}_j} a_{ji} (\hat{v}_j - \hat{v}_i) \right) \quad (2.11)$$

$$\dot{\hat{\psi}}_j = - \sum_{i \in \mathcal{N}_j} a_{ji} (\hat{\psi}_j - \hat{\psi}_i) - \beta_\psi \text{sign} \left( \sum_{i \in \mathcal{N}_j} a_{ji} (\hat{\psi}_j - \hat{\psi}_i) \right) \quad (2.12)$$

where  $\beta_p > \max_{t \in (0, \infty)} \{\|p\dot{0}\|\}$ ,  $\beta_v > \max_{t \in (0, \infty)} \{\|\dot{v}0\|\}$ , and  $\beta_\psi > \max_{t \in (0, \infty)} \{\|\dot{\psi}0\|\}$ .

**Lemma 2.1.** *For the distributed estimators in (2.10)-(2.12), if the leader's information is globally reachable to all other vehicles,  $(\hat{p}_j, \hat{v}_j, \hat{\psi}_j)$  converges to  $(p_0, v_0, \psi_0)$  within a finite time  $T$ , i.e., after time  $T$ ,  $(\hat{p}_j, \hat{v}_j, \hat{\psi}_j) = (p_0, v_0, \psi_0)$ .*

### 2.2.2 Tracking Controller Design

In this step, we design a tracking controller for each vehicle. Considering the cascade structure of the system, a backstepping tracking controller is proposed in the following steps.

**Step 1:** The dynamics in (2.1)-(2.2) can be written as

$$m_j \ddot{p}_j + m_j g e_3 = f_j R_j e_3 + m_j d_{1j} \quad (2.13)$$

Since  $m_j$  is a constant, the passivity property holds for the system. Let

$$s_j = \dot{p}_j - \hat{\dot{p}}_j - \dot{h}_j + k_{1j}(p_j - \hat{p}_j - h_j)$$

where  $k_{1j}$  is positive, then

$$m_j \dot{s}_j = f_j R_j e_3 + m_j d_{1j} - m_j g e_3 - m_j (\ddot{p}_j + \ddot{h}_j) + m_j k_{1j} (\dot{p}_j - \hat{\dot{p}}_j - \dot{h}_j).$$

Since  $m_j$  and  $d_{1j}$  are unknown, we use a neural network to approximate the unknown terms.

Choose the basis function of the neural networks as  $Y_{1j}$ , we have

$$m_j d_{1j} - m_j g e_3 - m_j (\ddot{p}_j + \ddot{h}_j) + m_j k_{1j} (\dot{p}_j - \hat{\dot{p}}_j - \dot{h}_j) = Y_{1j} W_{1j} + \epsilon_{1j} \quad (2.14)$$

where  $W_{1j}$  is an ideal constant weight vector and  $\epsilon_{1j}$  is the residue error vector. If the basis function is well chosen and the number of nodes is large enough,  $\|\epsilon_{1j}\| \leq c_{1j}$  for a given positive constant  $c_{1j}$ . So,

$$m_j \dot{s}_j = f_j R_j e_3 + Y_{1j} W_{1j} + \epsilon_{1j}. \quad (2.15)$$

We choose a Lyapunov function

$$V_{1j} = \frac{1}{2} m_j s_j^T s_j + \frac{1}{2} \gamma_{1j} (W_{1j} - \hat{W}_{1j})^T (W_{1j} - \hat{W}_{1j})$$

where  $\gamma_{1j}$  is a positive constant and  $\hat{W}_{1j}$  is an estimate of  $W_{1j}$ . Then,

$$\dot{V}_{1j} = s_j^\top (f_j R_j e_3 + Y_{1j} \omega_{1j} + \epsilon_{1j}) - \gamma_{1j} (W_{1j} - \widehat{W}_{1j}) \widehat{W}_{1j}.$$

If  $f_j R_j e_3$  were control input, we choose the virtual control input as

$$\alpha_j = \begin{bmatrix} \alpha_{1j} \\ \alpha_{2j} \\ \alpha_{3j} \end{bmatrix} = -k_2 s_j - Y_1 \widehat{W}_{1j} - c_{1j} \text{sign}(s_j) \quad (2.16)$$

and the update law of  $W_{1j}$  is

$$\dot{\widehat{W}}_{1j} = \gamma_{1j}^{-1} Y_{1j}^\top s_j \quad (2.17)$$

With the aid of the virtual control input, we have

$$\dot{V}_{1j} = s_j^\top (f_j R_j e_3 - \alpha_j) - k_2 s_j^\top s_j + s_j^\top \epsilon_{1j} - c_{1j} s_j^\top \text{sign}(s_j) \quad (2.18)$$

$$\leq s_j^\top (f_j R_j e_3 - \alpha_j) - k_2 s_j^\top s_j \quad (2.19)$$

**Step 2:** In this step, we find  $f_j$  and virtual control inputs  $\varphi_{dj}$  and  $\theta_{dj}$  for  $\varphi_j$  and  $\theta_j$ . We choose

$$f_j = \|\alpha_j\|. \quad (2.20)$$

Let  $f_j e_3 = R^\top(\Theta_{dj})\alpha_j$  and  $\psi_{dj} = \widehat{\psi}_j$ , simple calculation gives

$$\alpha_{1j}c\theta_{dj}c\psi_{dj} + \alpha_{2j}c\theta_{dj}s_{dj}\psi_{dj} - \alpha_{3j}s\theta_{dj} = 0 \quad (2.21)$$

$$\alpha_{1j}(s\theta_{dj}c\psi_{dj}s\varphi_{dj} - s\psi_{dj}c\varphi_{dj}) + \alpha_{2j}(s\theta_{dj}s\psi_{dj}s\varphi_{dj} + c\psi_{dj}c\varphi_{dj}) + \alpha_{3j}c\theta_{dj}s\varphi_{dj} = 0 \quad (2.22)$$

$$\alpha_{1j}(s\theta_{dj}c\psi_{dj}c\varphi_{dj} + s\psi_{dj}s\varphi_{dj}) + \alpha_{2j}(s\theta_{dj}s\psi_{dj}c\varphi_{dj} - c\psi_{dj}s\varphi_{dj}) + \alpha_{3j}c\theta_{dj}c\varphi_{dj} = f \quad (2.23)$$

where  $c\theta_{dj} = \cos\theta_{dj}$  and  $s\theta_{dj} = \sin\theta_{dj}$ . From (2.21) we have

$$\theta_{dj} = \arctan \left( \frac{\alpha_{1j}\cos\varphi_{dj} + \alpha_{2j}\sin\varphi_{dj}}{\alpha_{3j}} \right) \quad (2.24)$$

(2.23)  $\times \sin\varphi_{dj}$  - (2.22)  $\times \cos\varphi_{dj}$  yields

$$f_j \sin\varphi_{dj} = \alpha_{1j} \sin\psi_{dj} - \alpha_{2j} \cos\psi_{dj}.$$

From this equation, we choose

$$\phi_{dj} = \arcsin \left( \frac{\alpha_{1j}\sin\varphi_{dj} - \alpha_{2j}\cos\varphi_{dj}}{\|\alpha_j\|} \right) \quad (2.25)$$

With the aid of the virtual control input  $\Theta_{dj} = (\psi_{dj}, \varphi_{dj}, \psi_{dj})$ , (2.15) can be written as

$$\begin{aligned} m_j \dot{s}_j = & -k_{2j}s_j + Y_j(\hat{m}_j - m_j) - k_{3j}\text{sign}(s_j) + m_j d_{1j} \\ & + \|\alpha_j\| R(\Theta_{dj})(R(\Theta_j - \Theta_{dj}) - I_3)e_3 \end{aligned} \quad (2.26)$$

**Step 3:** In this step, we design the virtual control for  $\omega_j$  such that (2.8)-(2.9) are satisfied and the Euler angles  $(\varphi_j, \theta_j, \psi_j)$  are in the restrict regions in (2.6). Let

$$\xi_j = \begin{bmatrix} \tan\phi_j - \tan\phi_{d_j} \\ \tan\theta_j - \tan\theta_{d_j} \\ \tan\frac{\varphi}{2} - \tan\frac{\varphi_{d_j}}{2} \end{bmatrix} \quad (2.27)$$

then,

$$\dot{\xi}_j = G(\Theta_j)W(\Theta_j)\omega_j - G(\Theta_{d_j})\dot{\Theta}_{d_j} \quad (2.28)$$

where

$$G(\Theta_j) = \text{diag} \left( \left[ \frac{1}{\cos^2\phi_j}, \frac{1}{\cos^2\theta_j}, \frac{1}{2\cos^2\frac{\varphi_j}{2}} \right] \right)$$

It is obvious that  $\Theta_j$  is in the regions in (2.6) and (2.9) holds if  $\xi_j$  is bounded and converges to zero. To design a virtual controller for  $\omega_j$ , we choose a Lyapunov function

$$V_{2j} = \frac{1}{2} \xi_j^T \xi_j.$$

Then,

$$\dot{V}_{2j} = \xi_j^T (G(\Theta_j)W(\Theta_j)\omega_j - G(\Theta_{d_j})\dot{\Theta}_{d_j})$$

Choose the virtual controller of  $\omega_j$  as

$$\eta_j = (G(\Theta_j)W(\Theta_j))^{-1}(-k_{\Theta_j}\zeta_j + G(\Theta_{dj})\dot{\Theta}_{dj}) \quad (2.29)$$

where  $k_{\Theta_j}$  is a positive constant. If  $\omega_j = \eta_j$ ,

$$\dot{V}_{2j} = -\xi_j^T k_{\Theta_j} \xi_j \leq 0$$

which means that  $\xi_j$  exponentially converges to zero.

In (2.29), the inverse of  $G(\Theta_j)W(\Theta_j)$  always exists because  $\Theta_j$  is in the regions defined in (2.6) with the controllers defined in the next step.

**Step 4:** Since  $\omega_j$  is not a real control input and cannot be  $\eta_j$ , we let

$$\tilde{\omega}_j = \omega_j - \eta_j.$$

Then,

$$\dot{\xi}_j = -k_{\Theta_j}\xi_j + G(\Theta_j)W(\Theta_j)\tilde{\omega}_j \quad (2.30)$$

$$J_j\tilde{\omega}_j = S(J_j\omega_j)\omega_j + \tau_j - J_j\dot{\eta}_j + d_{2j} \quad (2.31)$$

Denote

$$J_j = \begin{bmatrix} J_{11j} & J_{12j} & J_{13j} \\ J_{21j} & J_{22j} & J_{23j} \\ J_{31j} & J_{32j} & J_{33j} \end{bmatrix}$$

and for any vector  $\zeta = [\zeta_1, \zeta_2, \zeta_3]^T \in R^3$  we define an operator

$$\Gamma(\zeta) = \begin{bmatrix} \zeta_1 & \zeta_2 & \zeta_3 & 0 & 0 & 0 \\ 0 & \zeta_1 & 0 & \zeta_2 & \zeta_3 & 0 \\ 0 & 0 & \zeta_1 & 0 & \zeta_2 & \zeta_3 \end{bmatrix}$$

then

$$J_j \zeta = \Gamma(\zeta) a_j$$

where  $a_j = [J_{11j}, J_{12j}, J_{13j}, J_{22j}, J_{23j}, J_{33j}]^T$  is a collection of all elements of  $J_j$ . Equation (2.31) can be written as

$$J_j \dot{\omega}_j = \tau_j - [S(\omega_j)\Gamma(\omega_j) + \Gamma(\dot{\eta}_j)]a_j + d_{2j}. \quad (2.32)$$

Since  $a_j$  and  $d_{2j}$  are unknown, we use a neural network to learn them. We choose a basis function  $Y_{2j}$  to approximate  $d_{2j} - [S(\omega_j)\Gamma(\omega_j) + \Gamma(\dot{\eta}_j)]a_j$ . Then

$$d_{2j} - [S(\omega_j)\Gamma(\omega_j) + \Gamma(\dot{\eta}_j)]a_j = Y_{2j}W_{2j} + \epsilon_{2j} \quad (2.33)$$

where  $W_{2j}$  is the ideal weight vector,  $\epsilon_{2j}$  is the residue error. For a given constant  $c_{2j}$ , we can choose  $Y_{2j}$  very well such that  $\|\epsilon_{2j}\| \leq c_{2j}$ . Then,

$$J_j \dot{\tilde{\omega}}_j = \tau_j + Y_{2j} W_{2j} + \epsilon_{2j}. \quad (2.34)$$

In order to propose an adaptive control law such that (2.8)-(2.9) are satisfied, we choose a Lyapunov function

$$V_{3j} = V_{2j} + \frac{1}{2} \tilde{\omega}_j^\top J_j \tilde{\omega}_j + \frac{1}{2} (W_{2j} - \hat{W}_{2j})^\top \gamma_{2j}^{-1} (W_{2j} - \hat{W}_{2j})$$

where  $\gamma_{2j}$  is a positive definite constant matrix and  $\hat{W}_{2j}$  is an estimate of  $W_{2j}$  and will be designed later. The derivative of  $V_{3j}$  along the solution of (2.30) and (2.34) is

$$\begin{aligned} \dot{V}_{3j} = & -\xi_j^\top k_{\Theta_j} \xi_j + \xi_j^\top G(\Theta_j) W(\Theta_j) \tilde{\omega}_j + \tilde{\omega}_j^\top \tau_j + \tilde{\omega}_j^\top \epsilon_{2j} + \tilde{\omega}_j^\top Y_{2j} W_{2j} - \\ & (W_{2j} - \hat{W}_{2j})^\top \gamma_{2j}^{-1} \dot{\hat{W}}_{2j}. \end{aligned}$$

We choose the control law and the update law as follows

$$\tau_j = -k_{\omega_j} \tilde{\omega}_j - [G(\Theta_j) W(\Theta_j)]^\top \xi_j + Y_{2j} \hat{W}_{2j} - c_{2j} \text{sign}(\tilde{\omega}_j) \quad (2.35)$$

$$\dot{\hat{W}}_{2j} = \gamma_{2j} Y_{2j}^\top \tilde{\omega}_j \quad (2.36)$$

where  $k_{\omega_j}$  is a positive constant. Then,

$$\dot{V}_{3j} = -\xi_j^\top k_{\Theta_j} \xi_j - \tilde{\omega}_j^\top k_{\omega_j} \tilde{\omega}_j \leq 0 \quad (2.37)$$

which means that  $\xi_j$  and  $\tilde{\omega}_j$  converges to zero and  $\hat{W}_{2j}$  is bounded.

Based on the above controller design procedure, we have the following results.

**Lemma 2.2.** *With the control input (2.35)-(2.36), (2.9) holds. Furthermore,  $\Theta_j - \Theta_{dj} \in L_2 \cap L_\infty$  and converges to zero.*

*Proof:* By the Lyapunov function  $V_{3j}$ , we have (2.37), which means that  $V_{3j}$  is bounded,  $\xi_j \in L_2$ , and  $\tilde{\omega}_j \in L_2$ . The boundedness of  $V_{3j}$  means that  $\xi_j, \tilde{\omega}_j \in L_\infty$ . So,  $\xi_j$  and  $\tilde{\omega}_j$  converge to zero, respectively. Therefore, (2.9) holds because the transformation  $\tan(\cdot)$  is one-to-one mapping for angles in  $(-\pi/2, \pi/2)$ .

By the mean value theorem, we have

$$\tan\phi_j - \tan\phi_{dj} = \frac{1}{\cos\phi_{c_j}} (\phi_j - \phi_{dj})$$

where  $\phi_{c_j}$  is a value between  $\phi_j$  and  $\phi_{dj}$ . Since  $\phi_j, \phi_{dj} \in \left(-\frac{\pi}{2}, \frac{\pi}{2}\right)$ ,  $\frac{1}{\cos^2\phi_{c_j}} \leq c_{\phi_j}$  where  $c_{\phi_j}$  is a positive constant. Since  $\xi_j \in L_2$ ,  $\phi_j - \phi_{dj} \in L_2$ . Similarly, it can be proved that  $\theta_j - \theta_{dj} \in L_2$  and  $\psi_j - \psi_{dj} \in L_2$ . Therefore,  $\Theta_j - \Theta_{dj} \in L_2 \cap L_\infty$ . So,  $\Theta_j - \Theta_{dj}$  converges to zero. Based on the above controller design procedure, we have the following results.

**Theorem 2.1.** *For the systems in (2.1)-(2.4) and a leader vehicle, if the information of the leader vehicle is globally reachable the control inputs  $(f_j, \tau_j)$  in (2.20) and (2.35) with the update laws in (2.17) and (2.36) ensure that (2.8)-(2.9) are satisfied and  $(\hat{W}_{1j}, \hat{W}_{2j})$  is bounded.*

*Proof:* By Lemma 2.2, eqn. (2.9) holds and  $\Theta_j - \Theta_{dj} \in L_2 \cap L_\infty$ . Furthermore, it can be shown that  $(R(\Theta_j - \Theta_{dj}) - I_3)e_3 \in L_2 \cap L_\infty$ . So,

$$\begin{aligned}
V_{1j} &\leq -k_{2j}s_j^\top s_j + s_j^\top \|\alpha_j\| R(\Theta_{dj})(R(\Theta_j - \Theta_{dj}) - I_3)e_3 \\
&\leq -k_{2j}s_j^\top s_j + 0.5k_{2j}s_j^\top s_j + \frac{1}{2k_{2j}} \|\alpha_j\|^2 (2(1 - c(\tilde{\theta}_j - \tilde{\theta}_{dj}))c(\phi_j - \phi_{dj}) + s^2(\phi_j - \phi_{dj})) \\
&= 0.5k_{2j}s_j^\top s_j + \frac{1}{2k_{2j}} \|\alpha_j\|^2 (2(1 - c(\tilde{\theta}_j - \tilde{\theta}_{dj}))c(\phi_j - \phi_{dj}) + s^2(\phi_j - \phi_{dj}))
\end{aligned}$$

Integrating both sides of the above inequality and noting that  $\Theta_{dj} - \Theta_j \in L_2 \cap L_\infty$ , it can be shown that  $s_j \in L_2 \cap L_\infty$ . Furthermore, it can be shown that  $s_j$  converges to zero. So, (2.8) holds.

**Remark 2.1.** *In order to implement the controllers in Theorem 2.1, derivatives of  $\eta$  and  $\Theta_d$  should be obtained. Calculation of them is tedious. To overcome this, the command filters proposed in [57] and [58] can be applied to estimate  $\dot{\eta}_j$  and  $\dot{\Theta}_{dj}$ . For given  $q_d$ , the command filter*

$$\dot{q}_1 = \omega_n q_2$$

$$\dot{q}_2 = -2\zeta\omega_n q_2 - \omega_n(q_1 - q_d)$$

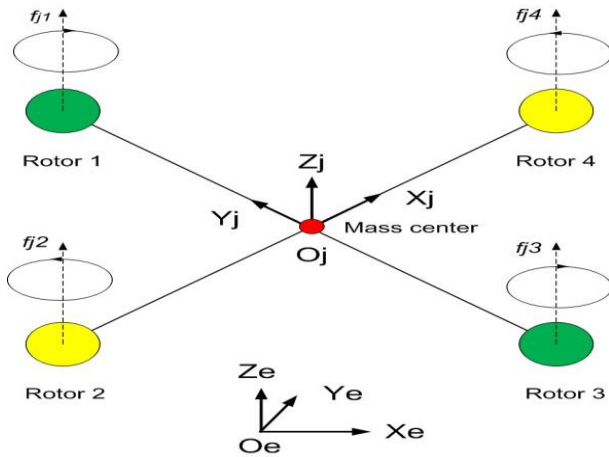


**Figure 2.6:** Configuration of a quadrotor

ensures that  $\|\omega_n q_2 - \dot{q}_d\|$  is small by letting  $0 < \zeta < 1$  and  $\omega_n (> 0)$  large.

### 2.3 Simulation Results

The proposed results can be applied to design distributed controllers for formation flying of multiple quadrotors. Considered five quadrotors. The dynamics of quadrotor  $j$  can be written as (2.1)(2.4), where the total thrust  $f_j$  and the generalized moment vector  $\tau_j$  are generated by the four rotors. For simplicity, we ignore the dynamics of each rotor and consider  $f_j$  and  $\tau_j$  as control inputs. In the simulation, it is assumed that  $m_j = 1\text{kg}$  and inertia tensor  $J_j = \text{diag}([1, 1, 1])\text{kg } m^2$ . In the controller design,  $m_j$  and  $J_j$  are not exactly known. However, it is known that  $m_j \in [0.8, 1.2]\text{kg}$ , i.e.,  $\bar{m} = 1.2\text{kg}$  and  $\underline{m} = 0.8\text{kg}$ .

Simulation results are presented to illustrate the effectiveness of the proposed controllers. Without loss of generality, for  $j$ -th quadrotor it is assumed that  $m_j = 1\text{kg}$  and inertia tensor  $J_j = \text{diag}([1, 1, 1])\text{kg } m^2$ . In the controllers,  $m_j$  and  $J_j$  are unknown and  $m_j \in [0.8, 1.2]$ .

In the simulation, it is assumed that the trajectory  $p_0$  and  $\psi_0$  of the leader quadrotor are

$$p_0(t) = \left[ 10 \left( 1 - \cos \frac{\pi t}{360} \right), 10 \sin \frac{\pi t}{360}, 1 \right]^T$$

$$\varphi^d = \frac{\pi}{3} \sin (0.01t)$$

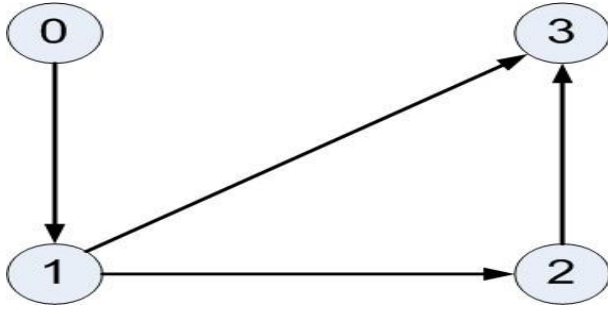


**Figure 2.7:** Communication graph between quadrotors

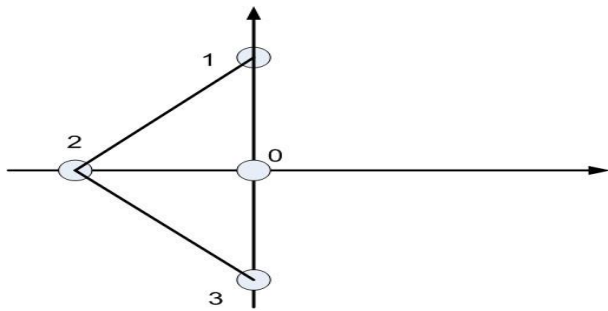


**Figure 2.8:** Desired formation

The communication directed graph is shown in Fig. 2.7. It can be verified that node 0 is globally reachable.

The desired formation for quadrotors is shown in Fig. 2.8, where  $h_0 = [0,0,0]^T$ ,  $h_1 = [0,15,0]^T$ ,  $h_2 = [-15,0,0]^T$ , and  $h_3 = [0,-15,0]^T$ .

Distributed control laws can be designed with the aid of the procedure in the last section. The simulation was done for a group of control parameters. Figs. 2.9-2.11 show the estimate errors  $p_0 - \hat{p}_j$ ,  $v_0 - \hat{v}_j$ , and  $\psi_0 - \hat{\psi}_j$  for  $1 \leq j \leq 3$ . It is shown that the estimates of the state of the leader converge to the desired value within finite time.

Fig. 2.12 shows the time response of  $p_j - h_j - (p_0 - h_0)$  for  $1 \leq j \leq 3$ . It is shown that the vehicles come into the desired formation and follow the leader vehicle. The time response of  $s_j$  is shown in Fig. 2.13, which shows that  $s_j$  converges to zero for  $1 \leq j \leq 3$ . The time response of  $\tilde{q}_j$  is shown in Fig. 2.14, which shows that the orientation of each vehicle converges to the orientation of the leader vehicle. Fig. 2.15 show the response of  $\tilde{\omega}_j$ . They are converge to zero.

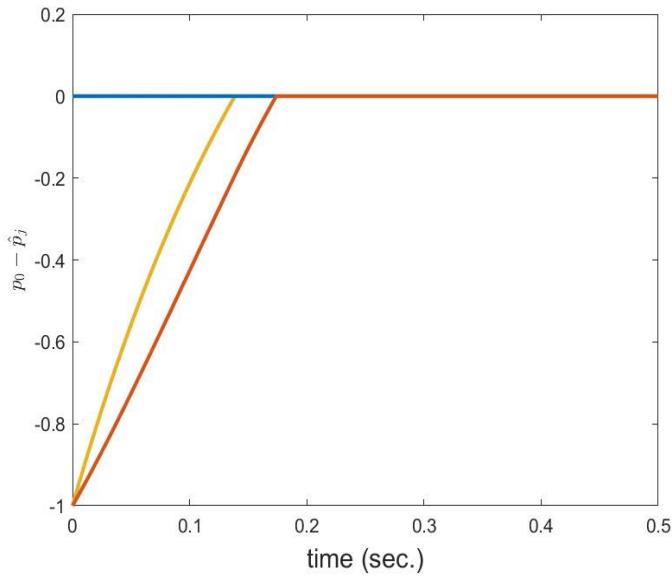


**Figure 2.9:** Estimate errors  $p_0 - \hat{p}_j$  for  $1 \leq j \leq 3$

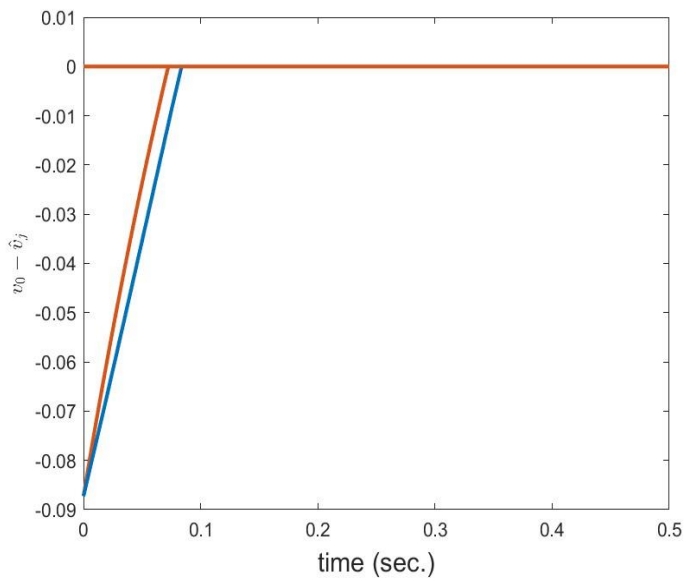


**Figure 2.10:** Estimate errors  $v_0 - \hat{v}_j$  for  $1 \leq j \leq 3$

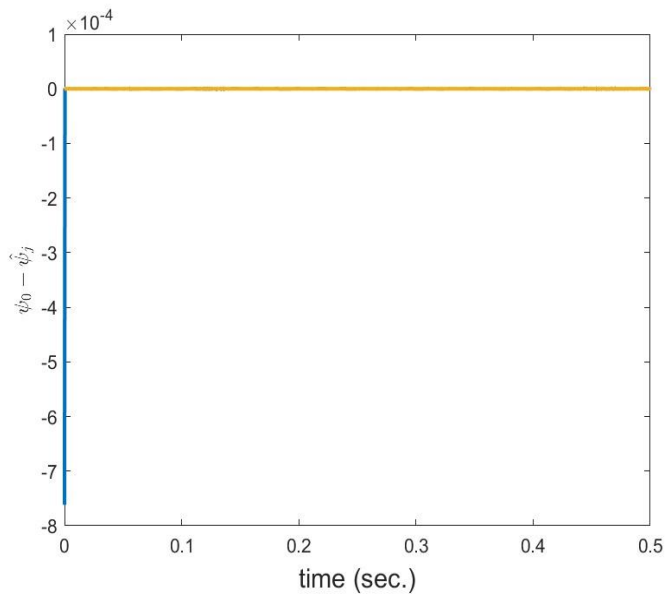


**Figure 2.11:** Estimate errors  $\psi_0 - \hat{\psi}_j$  for  $1 \leq j \leq 3$

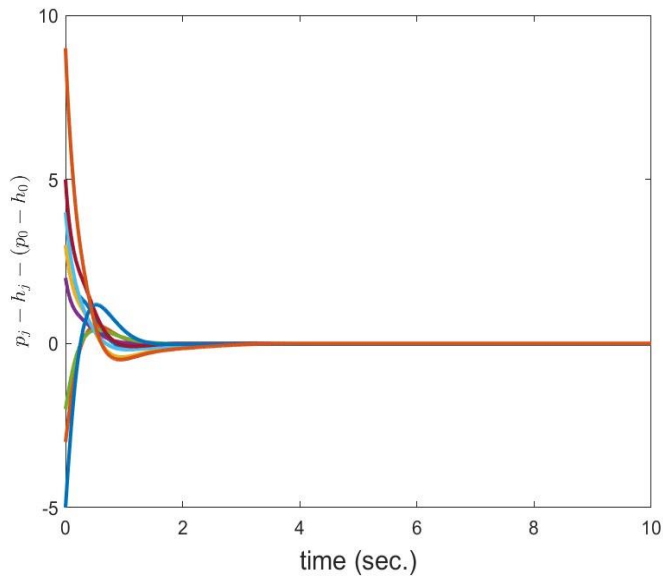


**Figure 2.12:** Tracking errors  $p_j - h_j - (p_0 - h_0)$  for  $1 \leq j \leq 3$

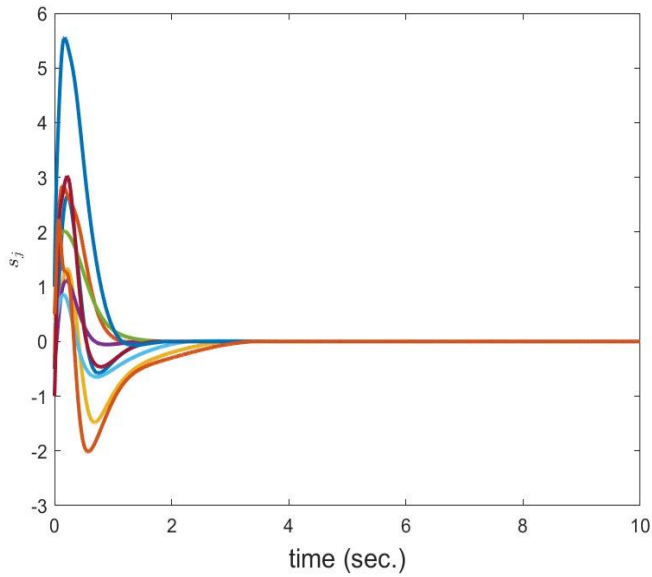


**Figure 2.13:** Tracking errors  $s_j$  for  $1 \leq j \leq 3$

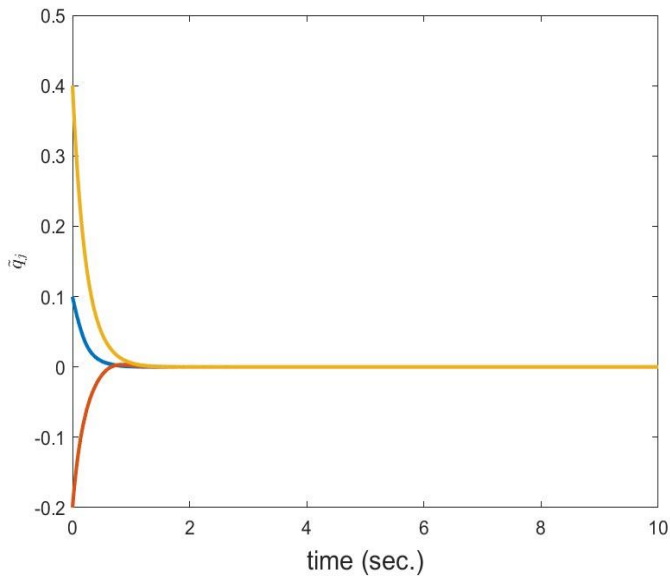


**Figure 2.14:** Tracking errors  $\tilde{q}_j$  for  $1 \leq j \leq 3$

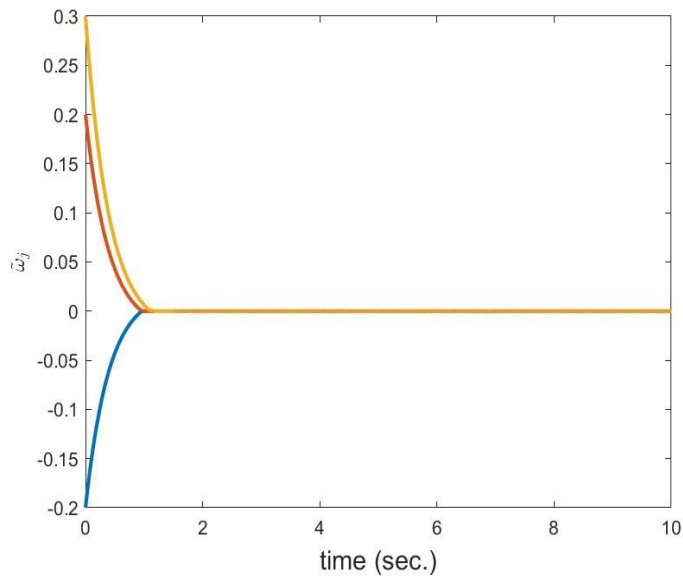


**Figure 2.15:** Tracking errors  $\tilde{\omega}_j$  for  $1 \leq j \leq 3$

## 2.4 Conclusion

This chapter considered the formation flying of multiple vehicles with a desired attitude in the presence of parametric and non-parametric uncertainty. With the aid of the distributed estimation, sliding mode control theory, and adaptive control theory, distributed control laws were proposed. Simulation results show the effectiveness of the proposed controllers for formation flying of three vehicles.

## CHAPTER III

### DISTRIBUTED TRACKING CONTROL OF MULTIPLE QUADROTORS WITH THE AID OF OPTIMAL CONTROL THEORY

#### 3.1 Introduction

Although there are many results on formation control of multiple quadrotors, how to improve the control performance is still challenging in the presence of uncertainty and coupling among neighboring quadrotors. Motivated by the research work in [53–55], in this chapter we study the optimal formation control of multiple quadrotors with parametric uncertainty and propose new distributed control laws with the aid of optimal control theory such that the formation errors converge to zero and the attitude of each quadrotor converges to a desired attitude.

#### 3.2 Problem Statement and Preliminaries

##### 3.2.1 Problem Statement

Consider  $m$  quadrotors. Under some assumptions, the kinematics and dynamics of  $j$ -th quadrotor are defined by

$$\dot{p}_j = v_j \tag{3.1}$$

$$\dot{v}_j = -g e_3 + \frac{1}{m_j} f_j R_j e_3 \quad (3.2)$$

$$\dot{R}_j = R S(\omega_j) \quad (3.3)$$

$$J_j \dot{\omega}_j = S(J_j \omega_j) \omega_j + \tau_j \quad (3.4)$$

where  $p_j$  and  $v_j$  are the position and the velocity of the mass center in the inertia frame, respectively,  $m_j$  is the mass of the  $j$ -th vehicle,  $g$  is the gravitational acceleration,  $e_3 = [0,0,1]^\top$ ,  $f_j \in \mathbb{R}$  is the total thrust,  $R_j = [b_{1j}, b_{2j}, b_{3j}]$  is the rotation matrix of the body frame with respect to the inertia frame,  $\omega_j$  is the angular velocity of the quadrotor in its body frame,  $J_j$  is the inertia moment of the quadrotor,  $S(\xi)$  for  $\xi = [\xi_1, \xi_2, \xi_3]^\top$  is a skew-symmetric matrix defined by

$$S(\xi) = \begin{bmatrix} 0 & -\xi_3 & \xi_2 \\ \xi_3 & 0 & -\xi_1 \\ -\xi_2 & \xi_1 & 0 \end{bmatrix}$$

and  $\tau_j = [\tau_{1j}, \tau_{2j}, \tau_{3j}]^\top$  is the torque input of the system.

For multiple quadrotors, there are information flows between them with the aid of sensors or wireless communication. Consider each quadrotor as a node. The communication between quadrotors is defined by a directed graph  $G = \{A, E\}$  where  $A$  is the node set and  $E$  is the edge set. If there is an edge  $e_{ij}$  in  $E$  it means that the information of node  $i$  is available to node  $j$ . Node  $i$  is called a neighbor of node  $j$  if the information of node  $i$  is available to node  $j$ . All neighbors of node  $j$  form a node set which is called the neighbor set of node  $j$  and is denoted by  $N_j$ . A directed path from node  $i$  to node  $j$  is a sequence of sets of edges that connect node  $i$  to node  $j$  by following their directions. Node  $i$  is said to be reachable to node  $j$  if there exists a directed path from node  $i$  to node  $j$ . Node  $i$  is said globally reachable if node  $i$  is reachable for every other node in  $A$ .

In this chapter, we assume there are  $m$  follower quadrotors and one leader quadrotor. The leader quadrotor is operated by a human operator and does not receive any information from the follower quadrotors. Without loss of generality, the leader quadrotor is labeled as node 0. The follower quadrotors are labeled by 1, 2, ...,  $m$ . The communication between  $m + 1$  quadrotors is defined by an augmented directed graph  $G^a = \{A^a, E^a\}$  where  $A^a = A \cup \{0\}$  and  $E^a$  is a union of  $E$  and the edges from node 0 to the followers.

For  $m$  follower quadrotors and a leader quadrotor, a desired formation can be defined by  $(m+1)$  vectors  $h_j \in R^3$  which may be constant vectors or time-varying vectors. We say  $(m+1)$  quadrotors are in the desired formation if

$$p_i - p_j = h_i - h_j$$

for any  $0 \leq i, j \leq m$ . We say  $m + 1$  quadrotors come into the desired formation if

$$\lim_{t \rightarrow \infty} [(p_i - h_i) - (p_j - h_j)] = 0$$

for any  $0 \leq i, j \leq m$ .

In the dynamics (3.1)-(3.4), the parametric uncertainty (i.e.,  $m_j$  and  $J_j$ ) is called the *system uncertainty*. For each quadrotor, it is unknown whether the leader quadrotor is a neighbor or not.

We say there is *information uncertainty* for each quadrotor.

In this chapter, we consider the following control problem.

**Formation flying with a leader:** For a leader quadrotor and  $m$  follower quadrotors, it is assumed that  $m_j$  and  $J_j$  are unknown for  $1 \leq j \leq m$ . It is given the position and the orientation of a

leader quadrotor and a desired formation defined by  $h_j$  for  $0 \leq j \leq m$ , the control problem is to design distributed *reinforcement learning based* state feedback controllers  $f_j$  and  $\tau_j$  using its own information and its neighbors' information such that

$$\lim_{t \rightarrow \infty} [(p_j - h_j) - (p_0 - h_0)] = 0 \quad (3.5)$$

$$\lim_{t \rightarrow \infty} [(b_{2j}(t) - b_{2,0}(t))] = 0 \quad (3.6)$$

for  $1 \leq j \leq m$ .

In the defined problem, (3.5) means that the  $(m+1)$  quadrotors come into the desired formation and (3.6) means that the  $Y$  axes of the body frames of  $m + 1$  quadrotors are parallel as time goes to infinity.

In order to solve the defined problem, the following assumptions are made.

**Assumption 3.1.** *The mass  $m_j$  of vehicle  $j$  is an unknown constant.*

**Assumption 3.2.** *The inertia matrix  $J_j$  of vehicle  $j$  is an unknown diagonal constant matrix and its elements on the diagonal are the element of a vector  $a_j$ .*

**Assumption 3.3.** *The communication graph  $G^a$  is a directed graph and the node 0 is globally reachable.*

**Assumption 3.4.**  $p_0(t)$  is smooth,  $\|\ddot{p}_0(t)\|$  and  $\|\ddot{p}_0\|$  are bounded.

**Assumption 3.5.**  $b_{2,0}(t)$  is smooth.  $\dot{b}_{2,0}$  and  $\ddot{b}_{2,0}$  are bounded.  $b_{2,0}^\top(t)b_{3,0}(t) = 0$  for any time

where  $b_{3,0}(t) = \frac{\ddot{p}_0(t) + ge_3}{\|\ddot{p}_0(t) + ge_3\|^2}$ .

The above assumptions are reasonable in practice.

The attitude of the  $j$ -th vehicle can be defined by a unit quaternion  $q_j = [\eta_j, \epsilon_j^\top]^\top$  where  $\eta_j \in \mathbb{R}$  and  $\epsilon_j \in \mathbb{R}^3$ . The relation between  $q_j$  and  $R_j$  is defined by

$$R_j = R(q_j) = I + 2\eta_j S(\epsilon_j) + 2S^2(\epsilon_j).$$

For the  $j$ -th vehicle, (3.3) can be written as

$$\dot{q}_j = \frac{1}{2} A(q_j) \omega_j \tag{3.7}$$

where

$$A(q_j) = \begin{bmatrix} -\epsilon_j^\top \\ \eta_j I + S(\epsilon_j) \end{bmatrix}. \tag{3.8}$$

### 3.3 Controller Design

In order to design distributed controllers, a multiple-step controller design procedure is proposed. In the first step, we design distributed estimators to estimate state of the leader vehicle using neighbors' information. In the second step, we estimate the unknown inertia parameters with the aid of data. Next, we design optimal controllers for each system such that the state of the vehicle asymptotically tracks the estimated state of the leader vehicle and minimize a cost function.

#### 3.3.1 Distributed Estimator Design

In this section, we apply the results in [56] to design distributed estimators. Let  $(\hat{p}_j, \hat{v}_j, \hat{\psi}_j)$  be the estimate of the leader's state  $(p_0, v_0, \psi_0)$ . Based on the results in [56], the distributed estimators for vehicle  $j$  are proposed as follows.

$$\hat{p}_j = \hat{v}_j \quad (3.9)$$

$$\begin{aligned} \hat{v}_j = & kv_j - \sum_{i \in \mathfrak{N}_j} a_{ji}(\hat{v}_j - \hat{v}_i) + k \sum_{i \in \mathfrak{N}_j} a_{ji}(\hat{p}_j - \hat{p}_i) - \beta_v \text{sign} \left( \sum_{i \in \mathfrak{N}_j} a_{ji}(\hat{v}_j - \hat{v}_i - \right. \\ & \left. k\hat{p}_j + k\hat{p}_i) \right) \end{aligned} \quad (3.10)$$

$$\dot{r}_j = - \sum_{i \in \mathfrak{N}_j} a_{ji}(r_j - r_i) - \beta_r \text{sign} \left( \sum_{i \in \mathfrak{N}_j} a_{ji}(r_j - r_i) \right) \quad (3.11)$$

where  $r_0 = b_{20} k > 0$ ,  $\beta_p > \max_{t \in (0, \infty)} \{\|\dot{p}_0\|\}$ ,  $\beta_v > \max_{t \in (0, \infty)} \{\|\dot{v}_0 + kp_0\|\}$ , and  $\beta_r > \max_{t \in (0, \infty)} \{\|\dot{b}_{20}\|\}$ .

**Lemma 3.1.** *For the distributed estimators in (3.9)-(3.11), if the leader's information is globally reachable to all other vehicles,  $(\hat{p}_j, \hat{v}_j, r_j)$  converges to  $(p_0, v_0, b_{20})$  within a finite time  $T$ , i.e., after time  $T$ ,  $(\hat{p}_j, \hat{v}_j, r_j) = (p_0, v_0, b_{20})$ .*

### 3.3.2 Parameter Estimation

In the dynamics (3.1)(3.4),  $m_j$  and  $J_j$  are unknown. They should be estimated with the aid of the measured data. To this end, we integrate (3.2) and (3.4) over time interval  $[t, t + \delta t]$  for some stabilizing controller  $f_j$  and  $\tau_j$ . Then,

$$m_j(v_j(t + \delta t) - v_j(t) + ge_3\delta t) = \int_t^{t+\delta t} f_j R_j e_3 d\tau$$

$$J_j(\omega_j(t + \delta t) - \omega_j(t)) = - \int_t^{t+\delta t} S(\omega_j) \text{diag}(\omega_j) d\tau \text{vec}(J_j) + \int_t^{t+\delta t} \tau_j d\tau$$

So,

$$m_j = \frac{(v_j(t+\delta t) - v_j(t) + ge_3\delta t)^\top \int_t^{t+\delta t} f_j R_j e_3 d\tau}{\|v_j(t+\delta t) - v_j(t) + ge_3\delta t\|^2} \quad (3.12)$$

$$vec(J_j) = \left( diag \left( \omega_j(t + \delta t) - \omega_j(t) \right) + \int_t^{t+\delta t} S(\omega_j) diag(\omega_j) d\tau \right)^{-1} \int_t^{t+\delta t} \tau_j d\tau \quad (3.13)$$

In (3.12) and (3.13), some terms should be nonsingular. To avoid singularity of these terms, one can integrate (3.2) and (3.4) over multiple time intervals.

In order to find  $m_j$  and  $J_j$ , one needs to integrate some signals. To this end, one can let these signals go through first integrators with zero initial conditions. If we define the following auxiliary variables

$$\dot{\xi}_{1j} = f_j R_j e_3, \xi_{1j}(t) = [0, 0, 0]^T \quad (3.14)$$

$$\dot{\xi}_{2j} = S(\omega_j) diag(\omega_j), \xi_{2j}(t) = \mathbf{0}_{3 \times 3} \quad (3.15)$$

$$\dot{\xi}_{3j} = \tau_j, \xi_{3j}(t) = \mathbf{0}_{3 \times 1} \quad (3.16)$$

then (3.12) and 3.13) can be written as

$$m_j = \frac{(v_j(t+\delta t) - v_j(t) + g e_3 \delta t)^T \xi_{1j}(t+\delta t)}{\|v_j(t+\delta t) - v_j(t) + g e_3 \delta t\|^2} \quad (3.17)$$

$$vec(J_j) = \left( diag \left( \omega_j(t + \delta t) - \omega_j(t) \right) + \xi_{2j}(t + \delta t) \right)^{-1} \xi_{3j}(t + \delta t) \quad (3.18)$$

### 3.3.3 Optimal Tracking Controller Design

In this step, we design a tracking controller for each vehicle with the aid of optimal control theory. With the aid of the distributed estimator and the estimates of  $m_j$  and  $J_j$ , for time  $t \geq T$  the estimator for system  $j$  can be written as

$$\dot{p}_j = v_j \quad (3.19)$$

$$\dot{v}_j = -g e_3 + \frac{1}{m_j} f_j R_j e_3 \quad (3.20)$$

Considering the cascade structure of the system, a backstepping tracking controller is proposed in the following steps when time  $t \geq T$ .

Step 1: Let

$$x_j = \begin{bmatrix} p_j - \hat{p}_j \\ v_j - \hat{v}_j \end{bmatrix}$$

then

$$\dot{x}_j = A_j x_j + B_j f_j R_j e_3 - B_j \hat{v}_j \quad (3.21)$$

where

$$A_j = \begin{bmatrix} 0_{3 \times 3} & I_{3 \times 3} \\ 0_{3 \times 3} & 0_{3 \times 3} \end{bmatrix}, B_j = \begin{bmatrix} 0_{3 \times 3} \\ I_{3 \times 3} \end{bmatrix}.$$

Define a cost function

$$J_{1j} = \int_0^{\infty} ((x_j^T Q_j x_j + [j f_j R_j e_3 - \hat{v}_j]^T N_j [f_j R_j e_3 - \hat{v}_j])$$

where  $Q_j$  and  $N_j$  are known positive definite matrices. We design a virtual control input  $\alpha_j$  for  $f_j R_j e_3$  such that  $x_j$  converges to zero and  $J_{1j}$  is minimized.

With the aid of the linear quadratic regulation (LQR) optimal control theory, the optimal controller is

$$\alpha_j = -K_j x_j + \hat{v}_j \quad (3.22)$$

where

$$K_j = N_j^{-1} B_j^T P_j \quad (3.23)$$

and  $P_j$  is a positive definite solution of the following Lyapunov function

$$(A_j - B_j K_j)^\top P_j + P_j (A_j - B_j K_j) + Q_j + K_j^\top N_j K_j = 0 \quad (3.24)$$

Substitute  $K_j$  to the above equation,  $P_j$  is the symmetric positive definite solution to the following well-known algebraic Riccati equation (ARE).

$$A_j^\top P_j + P_j A_j + Q_j - P_j B_j N_j^{-1} B_j^\top P_j = 0. \quad (3.25)$$

**Step 2:** In this step, we find  $f_j$  and the desired orientation  $R_j^d$  for  $j$ -th vehicle. Let

$$f_j R_j^d e_3 = \alpha_j \quad (3.26)$$

where  $R_j^d = [b_{1j}^d, b_{2j}^d, b_{3j}^d]$ , then

$$f_j = \|\alpha_j\| \quad (3.27)$$

$$b_{3j}^d = \frac{\dot{\alpha}_j}{\|\dot{\alpha}_j\|} \quad (3.28)$$

In (3.28),  $b_{3j}^d$  is not defined if  $\alpha_j = 0$ . In this case, we define  $b_{3j}^d$  as follows

$$b_{3j}^d = \frac{\dot{\alpha}_{2j}}{\|\dot{\alpha}_{2j}\|}$$

To define  $b_{1j}^d$  and  $b_{2j}^d$ , the information  $b_{2,0}$  is required. Based on the distributed estimator in (3.11), the estimate  $r_j$  of  $b_{20}$  for  $j$ -th vehicle is known. We choose

$$\bar{r}_j = r_j - r_j^\top b_{3j}^d b_{3j}^d \quad (3.29)$$

$$b_{2j}^d = \frac{\bar{r}_j}{\|\bar{r}_j\|} \quad (3.30)$$

$$b_{1j}^d = b_{2j}^d \times b_{3j}^d \quad (3.31)$$

The desired attitude of  $R_j$  is chosen as

$$R_j^d = [b_{1j}^d, b_{2j}^d, b_{3j}^d] \quad (3.32)$$

and the desired quaternion  $q_j^d = [\eta_j^d, (\epsilon_j^d)^\top]^\top$  is calculated by the equations (166)-(168) in [59]

which are omitted here. The desired angular velocity is calculated by

$$\omega_j^d = 2A(q_j^d)^\top \frac{dq_j^d}{dt}. \quad (3.33)$$

**Step 3:** Let the difference between  $q_j$  and  $q_j^d$  be

$$\tilde{q}_j = (q_j^d)^{-1} \otimes q_j = [\tilde{\eta}_j, -\tilde{\epsilon}_j^\top]^\top, \quad (3.34)$$

The derivative of  $\tilde{q}_j$  is

$$\dot{\tilde{q}}_j = \frac{1}{2}A(\tilde{q}_j)(\omega_j - \tilde{R}_j^\top \omega_j^d) \quad (3.35)$$

where  $\tilde{R}_j = (R_j^d)^\top R_j$ .

Let

$$\tilde{\omega}_j = \omega_j - \tilde{R}_j^\top \omega_j^d - K_1 \tilde{\epsilon}_j \quad (3.36)$$

where  $K_1$  is a symmetric positive definite constant matrix, then

$$\dot{\tilde{q}}_j = -\frac{1}{2} A(\tilde{q}_j) K_1 \tilde{\epsilon}_j \quad (3.37)$$

$$\begin{aligned} J_j \dot{\omega}_j &= S(J_j \omega_j) \omega_j + \tau_j - J_j \frac{d}{dt} (\tilde{R}_j^\top \omega_j^d) - J_j K_1 \dot{\tilde{\epsilon}}_j \\ &= -S(\tilde{\omega}_j) J_j \tilde{\omega}_j - S(\tilde{\omega}_j) J_j (\tilde{R}_j^\top \omega_j^d) J_j \tilde{\omega}_j \\ &\quad - S(\tilde{R}_j^\top \omega_j^d) J_j \tilde{R}_j^\top \omega_j^d + \tau_j - J_j \frac{d}{dt} (\tilde{R}_j^\top \omega_j^d) - J_j K_1 \dot{\tilde{\epsilon}}_j \end{aligned} \quad (3.38)$$

The following result has been proved in [60].

**Lemma 3.2.** *For the system in (3.37), if  $\tilde{\omega}_j$  is bounded and converges to zero, then  $\tilde{\epsilon}_j$  and  $\tilde{\omega}_j$  all converge to zero.*

With the aid of Lemma 3.2, we design control input  $\tau_j$  such that  $\tilde{\omega}_j$  converges to zero. First, we consider the optimal control problem of the following system

$$\dot{\tilde{\omega}}_j = -J_j^{-1} S(\tilde{\omega}_j) J_j \tilde{\omega}_j + J_j^{-1} \bar{\tau}_j \quad (3.39)$$

with a cost function

$$J_{2j} = \frac{1}{2} \int_0^\infty (\tilde{\omega}_j^\top K_2 \tilde{\omega}_j + \bar{\tau}_j^{-\top} K_2^{-1} \bar{\tau}_j) dt \quad (3.40)$$

where  $K_2$  is a symmetric positive definite matrix,  $\bar{\tau}_j$  is a virtue input.

Let the value function

$$V_j(\tilde{q}_j(t), \tilde{\omega}_j) = \frac{1}{2} \int_0^\infty (\tilde{\omega}_j^\top K_2 \tilde{\omega}_j + \tau_j^{-\top} K_2^{-1} \bar{\tau}_j) dt \quad (3.41)$$

The HJB equation is

$$H_j(\tilde{q}_j, \tilde{\omega}_j, \bar{\tau}_j) = \frac{1}{2} (\tilde{\omega}_j^\top K_2 \tilde{\omega}_j + \tau_j^{-\top} K_2^{-1} \bar{\tau}_j) + \frac{\partial V_j}{\partial \tilde{\omega}_j} (-J^{-1} S(\tilde{\omega}_j) J \tilde{\omega}_j + J^{-1} \bar{\tau}_j) \quad (3.42)$$

The optimal control is

$$\bar{\tau}_j^* = -k_1 \tilde{\epsilon}_j - K_2 J^{-1} \left[ \frac{\partial V_j}{\partial \tilde{\omega}_j} \right]^\top \quad (3.43)$$

and the value function corresponding to  $\bar{\tau}_j^*$  is

$$V_j^* = \frac{1}{2} \tilde{\omega}_j^\top J \tilde{\omega}_j. \quad (3.44)$$

With the aid of  $V_j^*$ , the optimal control input is

$$\bar{\tau}_j^* = -K_2 \tilde{\omega}_j \quad (3.45)$$

This means that with the aid of the Lyapunov function  $V_j^*$  the optimal control can be derived as

(3.45).

Since the equation (3.38) and equation (3.39) are similar, it is believed that  $V_j^*$  is a sub-optimal value function for the optimal control of systems (3.38) with the cost function (3.40). We choose a Lyapunov function

$$\bar{V}_j = V_j^* \quad (3.46)$$

The derivative of  $\bar{V}_j$  is

$$\begin{aligned} \dot{\bar{V}}_j &= \tilde{\omega}_j^\top J \dot{\tilde{\omega}}_j \\ &= \tilde{\omega}_j^\top (-S(\tilde{\omega}_j)J_j \tilde{\omega}_j - S(\tilde{\omega}_j)J_j \tilde{R}_j^\top \omega_j^d - S(\tilde{R}_j^\top \omega_j^d)J_j \tilde{\omega}_j \\ &\quad - S(\tilde{R}_j^\top \omega_j^d)J_j \tilde{R}_j^\top \omega_j^d + \tau_j - J_j \frac{d}{dt}(\tilde{R}_j^\top \omega_j^d) - J_j K_1 \dot{\tilde{\epsilon}}_j) \end{aligned} \quad (3.47)$$

Choose the control input

$$\begin{aligned} \tau_j &= -K_2 \tilde{\omega}_j + S(\tilde{\omega}_j)J_j \tilde{\omega}_j + S(\tilde{\omega}_j)\tilde{R}_j^\top \omega_j^d + S(\tilde{R}_j^\top \omega_j^d)J_j \tilde{\omega}_j \\ &\quad + S(\tilde{R}_j^\top \omega_j^d)J_j \tilde{R}_j^\top \omega_j^d + J_j \frac{d}{dt}(\tilde{R}_j^\top \omega_j^d) + J_j K_1 \dot{\tilde{\epsilon}}_j \end{aligned} \quad (3.48)$$

then

$$\dot{\bar{V}}_j = -\tilde{\omega}_j^\top K_2 \tilde{\omega}_j. \quad (3.49)$$

It can be shown that  $\tilde{\omega}_j$  converges to zero.

Based on the above controller design procedure, we have the following results.

**Theorem 3.1.** *For the systems in (3.1)-(3.4) and a leader vehicle, if the information of the leader vehicle is globally reachable the control inputs  $(f_j, \tau_j)$  in (3.27) and (3.48) ensure that (3.5)-(3.6) are satisfied.*

*Proof:* With the aid of (3.49), it can be proved that  $\tilde{\omega}_j$  is bounded and converges to zero. By Lemma 3.2,  $\tilde{\epsilon}_j$  converges to zero. So, eqn. (3.6) is satisfied.

With the aid of the above design, the algorithm for control is as follows.

**Control Algorithm:**

1. Initialization: Apply a control input  $(F_j, \tau_j)$  for a small amount of time. Based on the measured data, calculate  $m_j$  and  $J_j$  using (3.12)-(3.13).
2. On-line Control: Apply the control law  $f_j$  and  $\tau_j$  in (3.28) and (3.48) where  $(\hat{p}_j, \hat{v}_j, r_j)$  are defined in (3.9)-(3.11).

**Remark 3.1.** *In order to implement the controllers in Theorem 3.1, derivatives of some terms should be obtained. Calculation of them is tedious. To overcome this, the command filters proposed in [57] and [58] can be applied to estimate the derivatives. For a given  $q_d$ , the command filter*

$$\dot{q}_1 = \omega_n q_2$$

$$\dot{q}_2 = -2\zeta\omega_n q_2 - \omega_n(q_1 - q_d)$$

*ensures that  $\|\omega_n q_2 - \dot{q}_d\|$  is small by letting  $0 < \zeta < 1$  and  $\omega_n (> 0)$  large.*

### 3.4 Simulation Results

The proposed results can be applied to design distributed controllers for formation flying of multiple quadrotors. Considered five quadrotors. The dynamics of quadrotor  $j$  can be written as (2.1)-(2.4), where the total thrust  $f_j$  and the generalized moment vector  $\tau_j$  are generated by the four rotors. For simplicity, we ignore the dynamics of each rotor and consider  $f_j$  and  $\tau_j$  as control inputs.

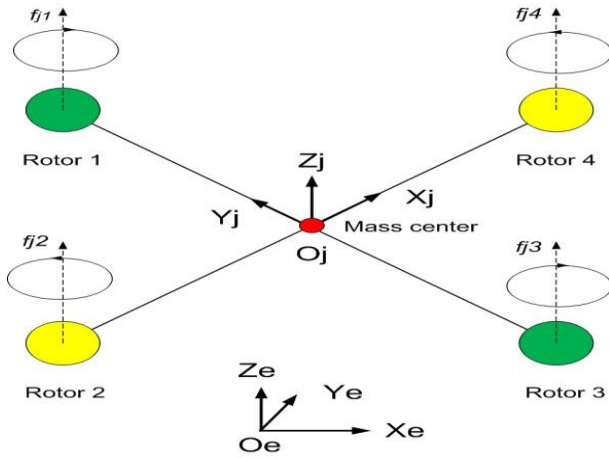


**Figure 3.1:** Configuration of a quadrotor

In the simulation, it is assumed that  $m_j = 1\text{kg}$  and inertia tensor  $J_j = \text{diag}([1, 1, 1])\text{kg } m^2$ . In the controller design,  $m_j$  and  $J_j$  are not exactly known. However, it is known that  $m_j \in [0.8, 1.2]\text{kg}$ , i.e.,  $\underline{m} = 0.8\text{kg}$  and  $\bar{m} = 1.2\text{kg}$ . Simulation results are presented to illustrate the effectiveness of the proposed controllers. Without loss of generality, for  $j$ -th quadrotor it is assumed that  $m_j = 1\text{kg}$  and inertia tensor  $J_j = \text{diag}([1, 1, 1])\text{kg } m^2$ . In the controllers,  $m_j$  and  $J_j$  are unknown and  $m_j \in [0.8, 1.2]$ .

In the simulation, it is assumed that the trajectory  $p_0$  and  $\psi_0$  of the leader quadrotor are

$$p_0(t) = \left[ 100 \cos \frac{t}{20}, 100 \sin \frac{t}{20}, 10 - 10 \exp(-0.1t) \right]^T$$

$$b_{2,0} = \left[ \sin \left( \pi * \frac{t}{60} \right), \cos \left( \pi * \frac{t}{360} \right), 0 \right]^T$$

The communication directed graph is shown in Fig. 3.2. It can be verified that node 0 is globally reachable. The desired formation for quadrotors is shown in Fig. 3.3, where  $h_0 = [0,0,0]^T$ ,  $h_1 = [0,15,0]^T$ ,  $h_2 = [-15,0,0]^T$ ,  $h_3 = [0,-15,0]^T$ , and  $h_4 = [15,0,0]^T$ .

Distributed control laws can be designed with the aid of the procedure in the last section. The simulation was done for one group of control parameters. Figs. 3.4-3.12 show the estimate errors  $p_0 - \hat{p}_j$ ,  $v_0 - \hat{v}_j$ , and  $b_{2,0} - r_j$  for  $1 \leq j \leq 3$ . It is shown that the estimates of the state of the leader converge to the desired value within finite time.

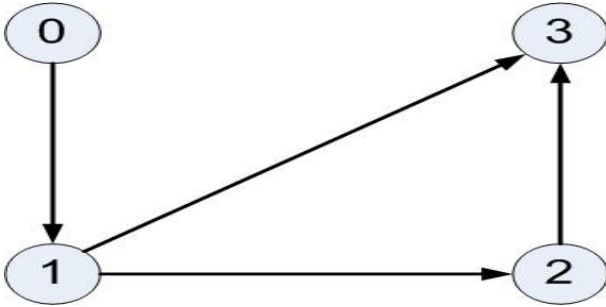


**Figure 3.2:** Communication graph between quadrotors

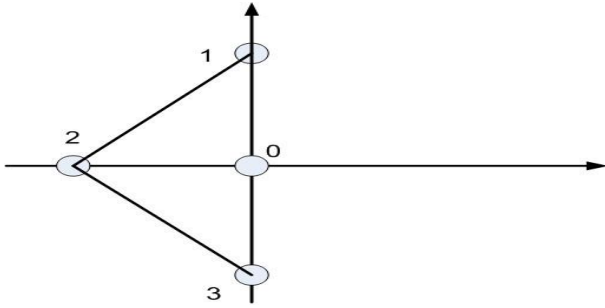


**Figure 3.3:** Desired formation

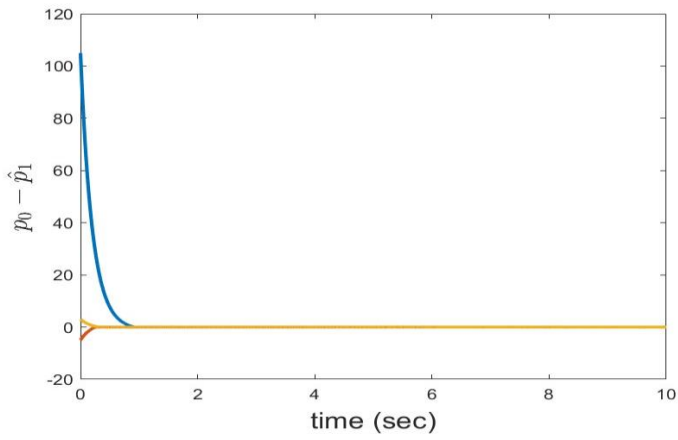


**Figure 3.4:** Estimation error  $p_0 - \hat{p}_1$ .

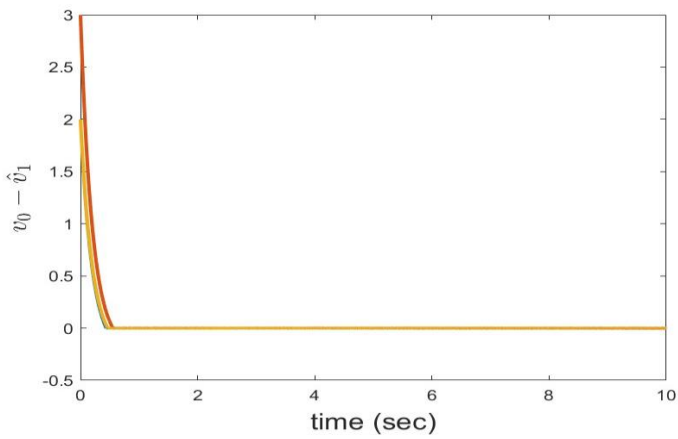


**Figure 3.5:** Estimation error  $v_0 - \hat{v}_1$ .

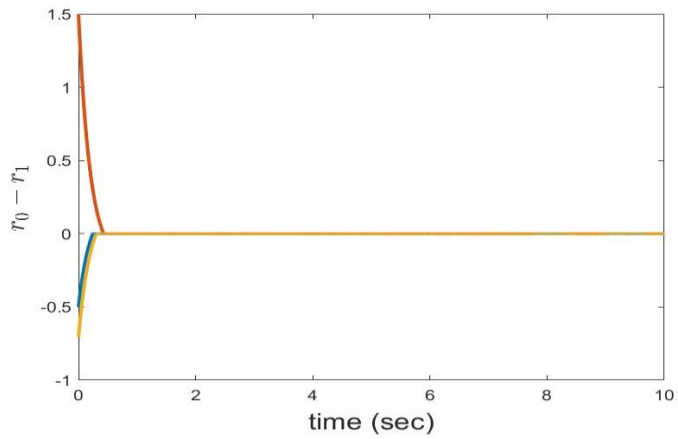


**Figure 3.6:** Estimation error  $b_{2,0} - r_{1}$ .

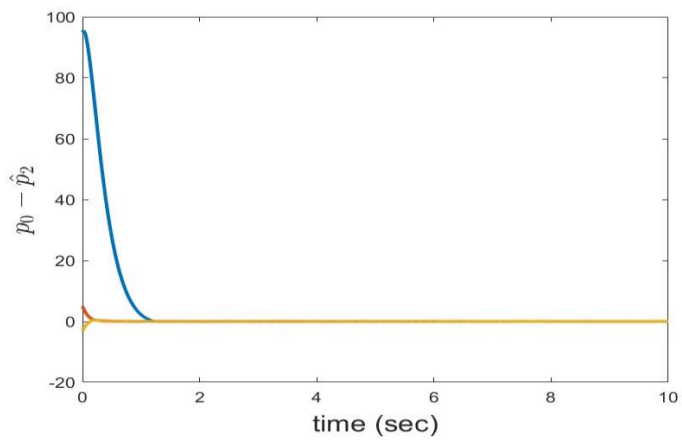


**Figure 3.7:** Estimation error  $p_0 - p_{2}$ .

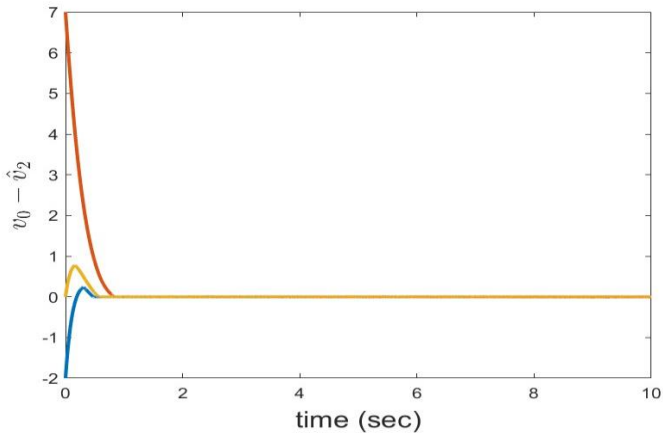


**Figure 3.8:** Estimation error  $v_0 - \hat{v}_2$ .

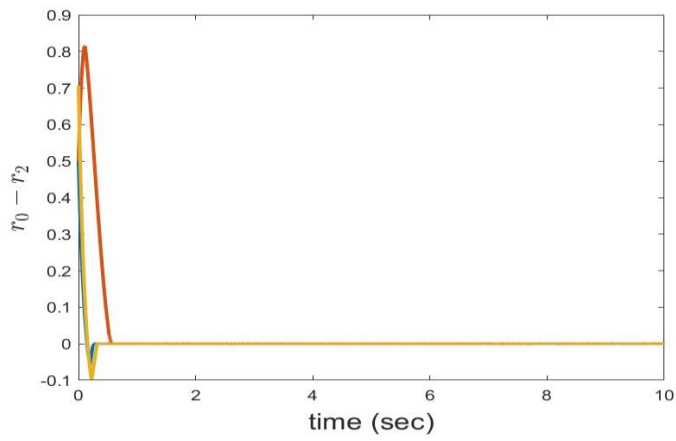


**Figure 3.9:** Estimation error  $b_{2,0} - \hat{r}_2$ .

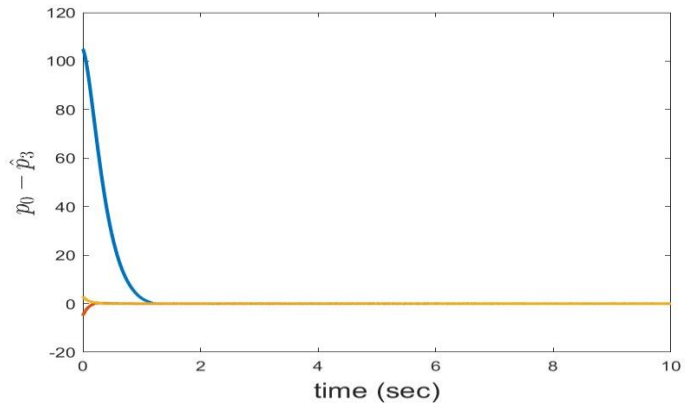


**Figure 3.10:** Estimation error  $p_0 - \hat{p}_3$ .

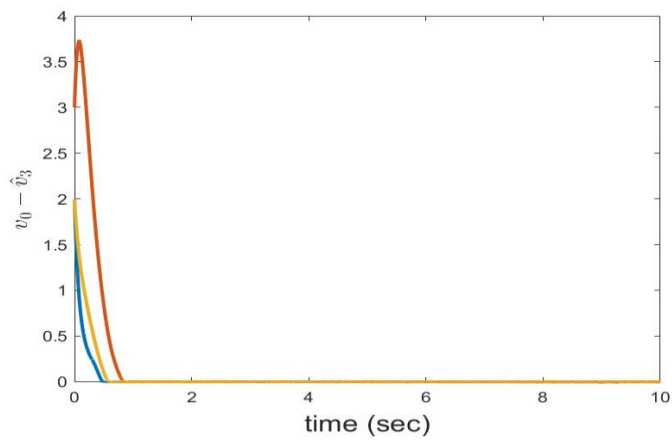


**Figure 3.11:** Estimation error  $v_0 - \hat{v}_3$ .

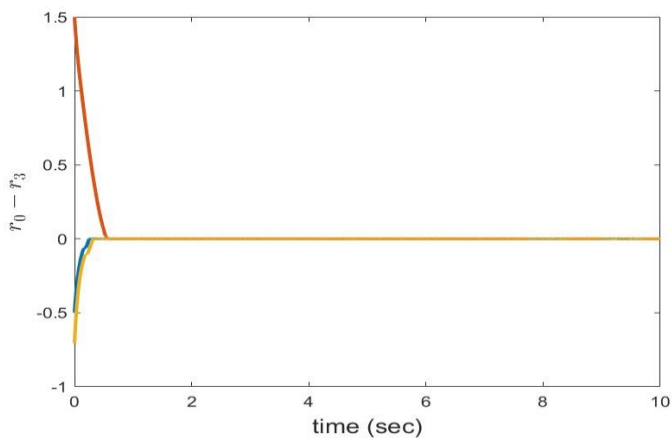


**Figure 3.12:** Estimation error  $b_{2,0} - \hat{r}_3$ .

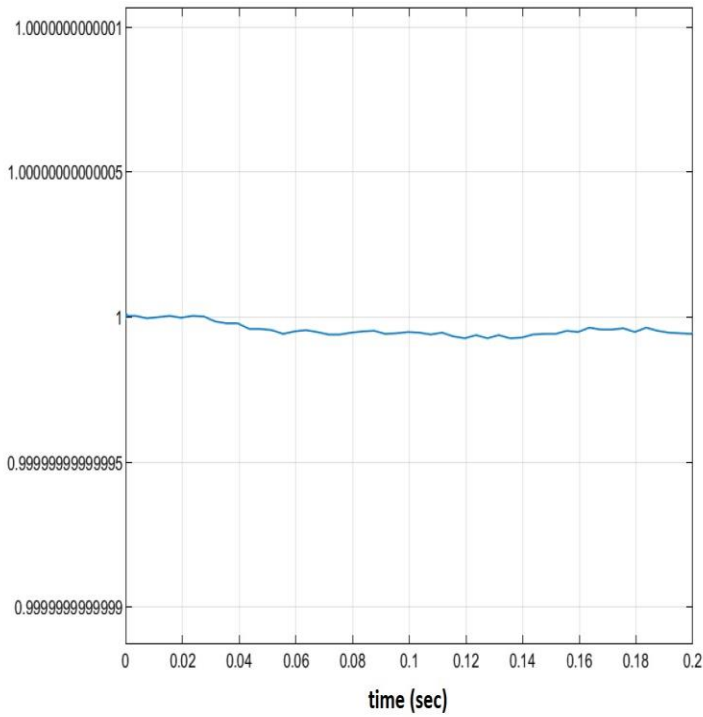


**Figure 3.13:** Time response of the estimate of  $m_j$ .

Figs. (3.13)-(3.14) show the estimates of  $m_j$  and  $J_j$ . It is shown that the estimates are very close to their real values.

Figs. 3.15-3.17 show the time response of  $p_j - h_j - (p_0 - h_0)$  for  $1 \leq j \leq 3$ . It is shown that the vehicles come into the desired formation and follow the leader vehicle. Figs. 3.18-3.20 show the time response of  $v_j - v_0$  for  $1 \leq j \leq 3$ . It is shown that the velocity of the vehicles converge to the desired velocity. Figs. 3.21-3.23 show the time response of  $q_j$  for  $1 \leq j \leq 3$ . It is shown that the orientation of the vehicles converge to the orientation of the lead vehicle. Figs. 3.24-3.26 show the time response of  $\omega_j$  for  $1 \leq j \leq 3$ . It is shown that the angular velocity of the vehicles converge to the desired angular velocity.

### 3.5 Conclusion

This chapter considered the formation flying of multiple vehicles with the aid of optimal control theory. The proposed approach integrates the distributed estimation, parameter identification, and

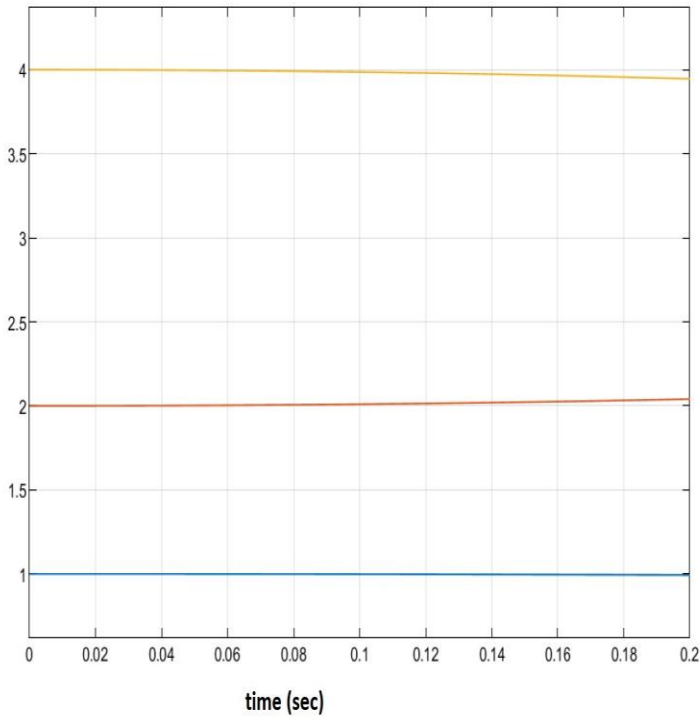


**Figure 3.14:** Time response of the estimate of  $J_j$ .

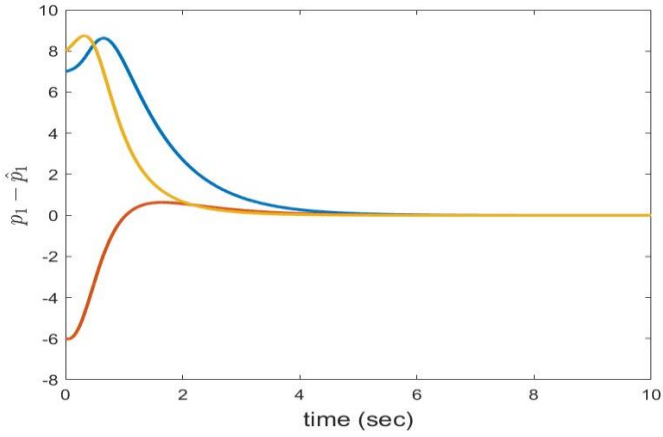


**Figure 3.15:** The tracking error  $p_1 - h_1 - (p_0 - h_0)$ .

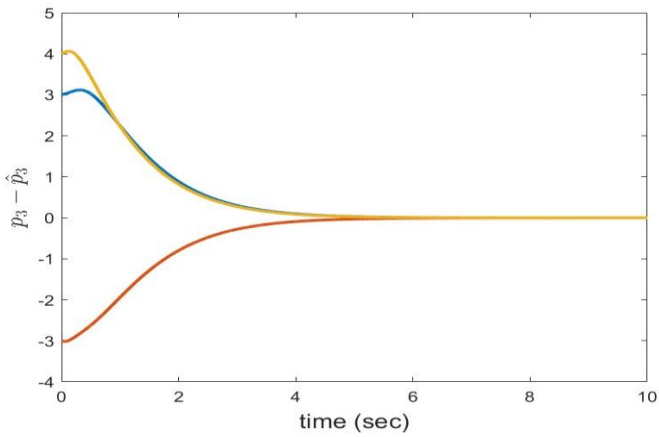


**Figure 3.16:** The tracking error  $p_2 - h_2 - (p_0 - h_0)$ .

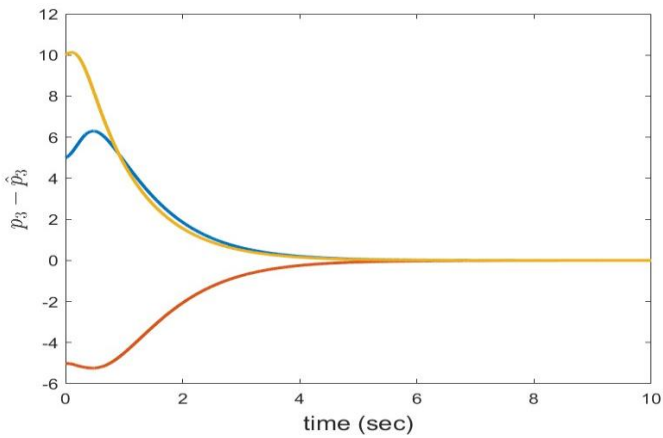


**Figure 3.17:** The tracking error  $p_3 - h_3 - (p_0 - h_0)$ .

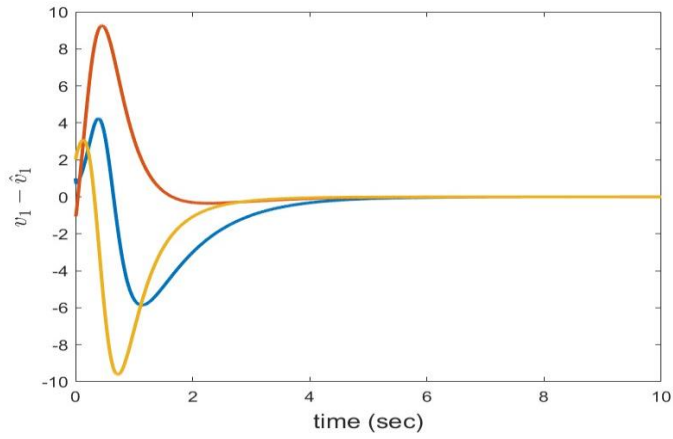


**Figure 3.18:** The tracking error  $v_1 - v_0$ .

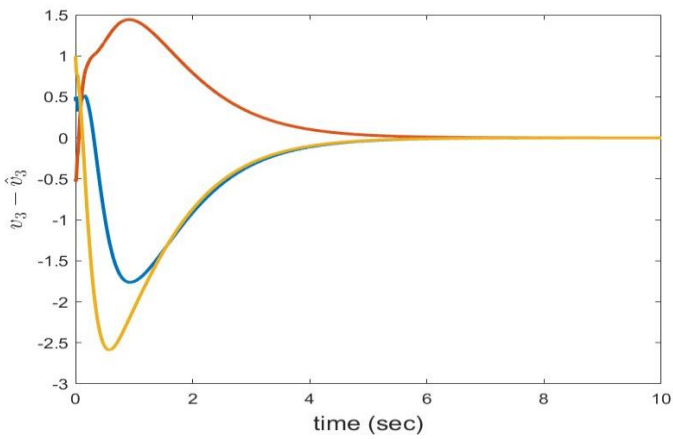


**Figure 3.19:** The tracking error  $v_2 - v_0$ .

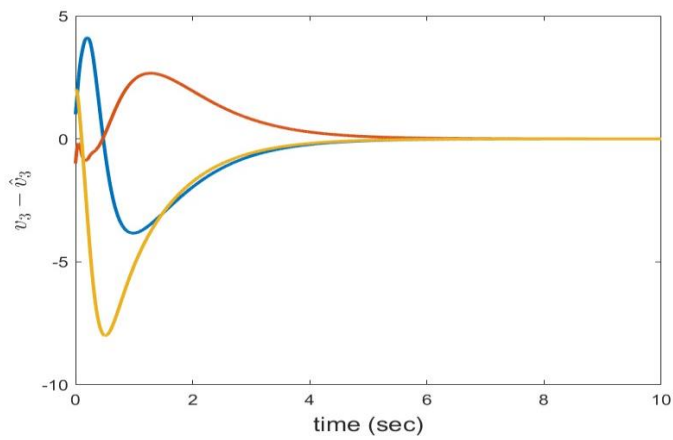


**Figure 3.20:** The tracking error  $v_3 - v_0$ .

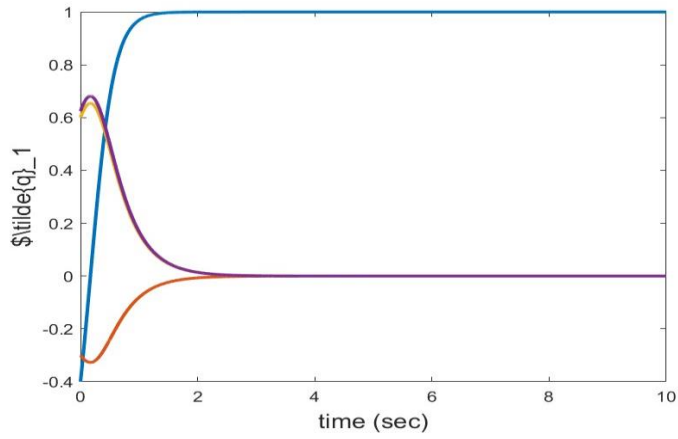


**Figure 3.21:** The tracking error  $q_{\tilde{1}}$ .

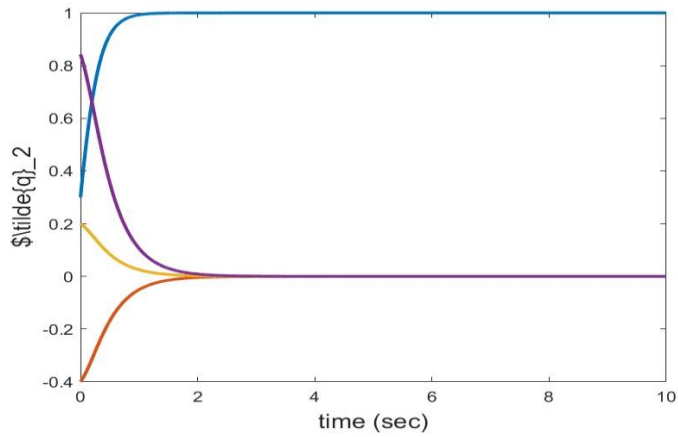


**Figure 3.22:** The tracking error  $q_{\tilde{2}}$ .

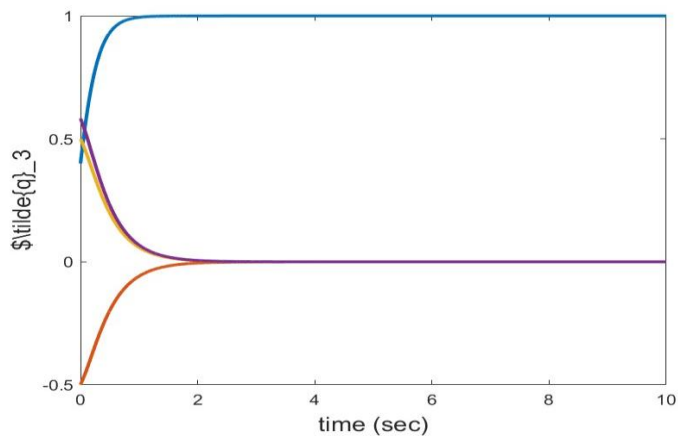


**Figure 3.23:** The tracking error  $q_{\tilde{3}}$ .

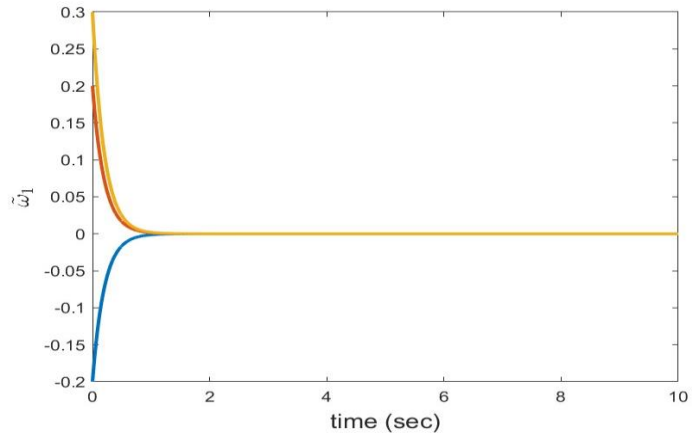


**Figure 3.24:** The tracking error  $\tilde{\omega}_1$ .

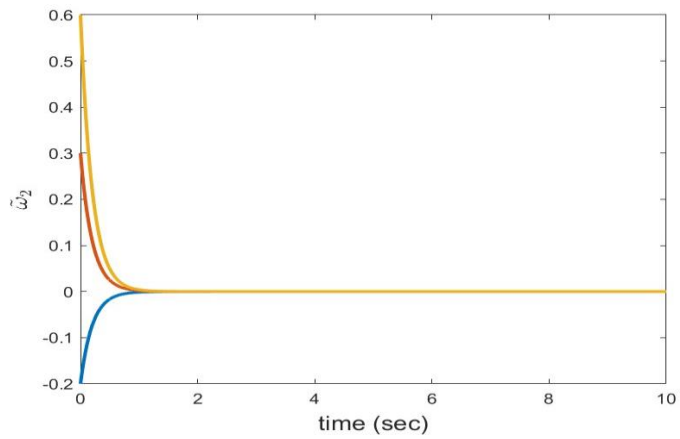


**Figure 3.25:** The tracking error  $\tilde{\omega}_2$ .

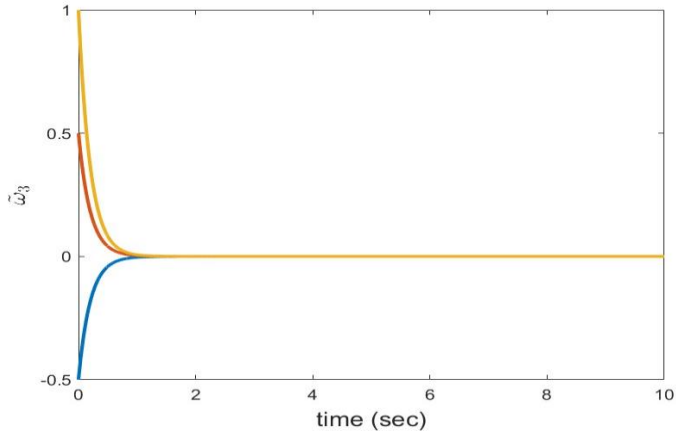


**Figure 3.26:** The tracking error  $\tilde{\omega}_3$ .

optimal tracking control. Simulation results show the effectiveness of the proposed controllers for formation flying of three vehicles.

## CHAPTER IV

### FUTURE WORK

In this thesis, we solved the formation flying of multiple quadrotors with the aid of distributed estimation, neural network approximation property, and optimal control theory. The obtained results are preliminary. Further research should be done on both research topics. In the future, the following research topics will be done.

- In this thesis, distributed controllers were design with the aid of the distributed estimation and the tracking controller design. The distributed estimation and the tracking control are separately steps. In the future, we will combine these two steps together.
- In this thesis, we studied the formation control of quadrotors. In the future, we will study the formation control of other types of vehicles, such as wheeled mobile robots, surface vehicles, etc.
- Reinforcement learning is a powerful tool in dealing with unknown environment. In the future, we will study distributed control of multiple vehicles with the aid of reinforcement learning instead of optimal control theory.
- Other distributed control problems.

## REFERENCES

- [1] A. Abdessameud and A. Tayebi, "Global trajectory tracking control of vtol-uavs without linear velocity measurements," *Automatica*, vol. 46, no. 6, pp. 1053 – 1059, 2010.
- [2] A. M. Zou, A. H. J. de Ruiter, and K. D. Kumar, "Finite-time attitude tracking control for rigid spacecraft with control input constraints," *IET Control Theory Applications*, vol. 11, no. 7, pp. 931–940, 2017.
- [3] A. Mokhtari, A. Benallegue, and B. Daachi, "Robust feedback linearization and gain infinity controller for a quadrotor unmanned aerial vehicle," in *2005 IEEE/RSJ International Conference on Intelligent Robots and Systems*, Aug 2005, pp. 1198–1203.
- [4] A. Tayebi, "Unit quaternion-based output feedback for the attitude tracking problem," *IEEE Transactions on Automatic Control*, vol. 53, no. 6, pp. 1516–1520, July 2008.
- [5] B. WIE and P. M. BARBA, "Quaternion feedback for spacecraft large angle maneuvers," *Journal of Guidance, Control, and Dynamics*, vol. 8, no. 3, pp. 360–365, 1985.
- [6] B. Zhao, B. Xian, Y. Zhang, and X. Zhang, "Nonlinear robust adaptive tracking control of a quadrotor uav via immersion and invariance methodology," *IEEE Transactions on Industrial Electronics*, vol. 62, no. 5, pp. 2891–2902, May 2015.
- [7] B. Zhao, B. Xian, Y. Zhang, and X. Zhang, "Nonlinear robust sliding mode control of a quadrotor unmanned aerial vehicle based on immersion and invariance method," *International Journal of Robust and Nonlinear Control*, vol. 25, no. 18, pp. 3714–3731, 2015.

- [8] B. Zhu and W. Huo, “Adaptive backstepping control for a miniature autonomous helicopter,” in 2011 50th IEEE Conference on Decision and Control and European Control Conference, Dec 2011, pp. 5413–5418.
- [9] C. G. Mayhew, R. G. Sanfelice, and A. R. Teel, “Quaternion-based hybrid control for robust global attitude tracking,” *IEEE Transactions on Automatic Control*, vol. 56, no. 11, pp. 2555–2566, Nov 2011.
- [10] C. Ha, Z. Zuo, F. B. Choi, and D. Lee, “Passivity-based adaptive backstepping control of quadrotor-type uavs,” *Robotics and Autonomous Systems*, vol. 62, no. 9, pp. 1305 – 1315, 2014, *intelligent Autonomous Systems*.
- [11] C. Hua, J. Chen, and Y. Li, “Leader-follower finite-time formation control of multiple quadrotors with prescribed performance,” *International Journal of Systems Science*, vol. 48, no. 12, pp. 2499–2508, 2017.
- [12] E. Lefeber, S. J. A. M. van den Eijnden, and H. Nijmeijer, “Almost global tracking control of a quadrotor uav on  $se(3)$ ,” in 2017 IEEE 56th Annual Conference on Decision and Control (CDC), Dec 2017, pp. 1175–1180.
- [13] E. Zhao, T. Chao, S. Wang, and M. Yang, “Finite-time formation control for multiple flight vehicles with accurate linearization model,” *Aerospace Science and Technology*, vol. 71, pp. 90 – 98, 2017.
- [14] G. Lafferriere, A. Williams, J. Caughman, and J. J. P. Veerman, “Decentralized control of vehicle formations,” *Systems and Control Letters*, vol. 53, pp. 899–910, 2005.
- [15] G. Lafferriere, J. Caughman, and A. Williams, “Graph theoretic methods in the stability of vehicle formations,” *Proc. of American Control Conf.*, pp. 3729–3734, 2004.
- [16] G. V. Raffo, M. G. Ortega, and F. R. Rubio, “An integral predictive/nonlinear  $h_\infty$  control structure for a quadrotor helicopter,” *Automatica*, vol. 46, no. 1, pp. 29 – 39, 2010.

- [17] H. Du, W. Zhu, G. Wen, Z. Duan, and J. LÅÆ, “Distributed formation control of multiple quadrotor aircraft based on nonsmooth consensus algorithms,” *IEEE Transactions on Cybernetics*, vol. 49, no. 1, pp. 342–353, 2019.
- [18] H. Gui and G. Vukovich, “Finite-time angular velocity observers for rigid-body attitude tracking with bounded inputs,” *International Journal of Robust and Nonlinear Control*, vol. 27, no. 1, pp. 15–38, 2017.
- [19] H. Liu, T. Ma, F. L. Lewis, and Y. Wan, “Robust formation control for multiple quadrotors with nonlinearities and disturbances,” *IEEE Transactions on Cybernetics*, vol. 50, no. 4, pp. 1362–1371, 2020.
- [20] H. Liu, Y. Tian, F. L. Lewis, Y. Wan, and K. P. Valavanis, “Robust formation tracking control for multiple quadrotors under aggressive maneuvers,” *Automatica*, vol. 105, pp. 179 – 185, 2019.
- [21] I.-H. Choi and H. Bang, “Adaptive command filtered backstepping tracking controller design for quadrotor unmanned aerial vehicle,” *Proceedings of the Institution of Mechanical Engineers, Part G: Journal of Aerospace Engineering*, vol. 226, pp. 483–497, 04 2011.
- [22] J. A. Farrell, M. Polycarpou, M. Sharma, and W. Dong, “Command filtered backstepping,” *IEEE Transactions on Automatic Control*, vol. 54, no. 6, pp. 1391–1395, June 2009.
- [23] J. A. Fax and R. M. Murray, “Information flow and cooperative control of vehicle formations,” *IEEE Trans. on Auto. Contr.*, vol. 49, pp. 1465–1476, 2004.
- [24] J. Hu and H. Zhang, “Immersion and invariance based command-filtered adaptive backstepping control of vtol vehicles,” *Automatica*, vol. 49, no. 7, pp. 2160 – 2167, 2013.
- [25] J. Lawton, R. W. Beard, and B. Young, “A decentralized approach to formation maneuvers,” *IEEE Trans. on Robotics and Automation*, vol. 19, no. 6, pp. 933–941, 2003.

- [26] J. P. Desai, J. P. Ostrowski, and V. Kumar, "Modeling and control of formations of nonholonomic mobile robots," *IEEE Trans. on Robotics and Automation*, vol. 17, pp. 905–908, 2001.
- [27] K. Alexis, G. Nikolakopoulos, and A. Tzes, "Switching model predictive attitude control for a quadrotor helicopter subject to atmospheric disturbances," *Control Engineering Practice*, vol. 19, no. 10, pp. 1195 – 1207, 2011.
- [28] K. Sugihara and I. Suzuki, "Distributed algorithms for formation of geometric patterns with many mobile robots," *J. of Robotic Systems*, vol. 13, no. 3, pp. 127–139, 1996.
- [29] L. Besnard, Y. B. Shtessel, and B. Landrum, "Quadrotor vehicle control via sliding mode controller driven by sliding mode disturbance observer," *Journal of the Franklin Institute*, vol. 349, no. 2, pp. 658 – 684, 2012, advances in Guidance and Control of Aerospace Vehicles using Sliding Mode Control and Observation Techniques.
- [30] L. Dou, C. Yang, D. Wang, B. Tian, and Q. Zong, "Distributed finite-time formation control for multiple quadrotors via local communications," *International Journal of Robust and Nonlinear Control*, vol. 29, no. 16, pp. 5588–5608, 2019.
- [31] L. Sun and Z. Zuo, "Nonlinear adaptive trajectory tracking control for a quad-rotor with parametric uncertainty," *Proceedings of the Institution of Mechanical Engineers, Part G: Journal of Aerospace Engineering*, vol. 229, no. 9, pp. 1709–1721, 2015.
- [32] L. Wang and H. Jia, "The trajectory tracking problem of quadrotor uav: Global stability analysis and control design based on the cascade theory," *Asian Journal of Control*, vol. 16, no. 2, pp. 574–588, 2014.
- [33] M. A. Lewis and K.-H. Tan, "High precision formation control of mobile robots using virtual structures," *Autonomous Robots*, vol. 4, pp. 387–403, 1997.

- [34] M. D. Shuster, "Survey of attitude representations," *Journal of the Astronautical Sciences*, 1993.
- [35] M. Mesbahi and F. Y. Hadaegh, "Formation flying control of multiple spacecraft via graphs, matrix inequalities, and switching," *AIAA J. of Guidance, Control, and Dynamics*, vol. 24, pp. 369–377, 2001.
- [36] M. Radmanesh and M. Kumar, "Flight formation of uavs in presence of moving obstacles using fast-dynamic mixed integer linear programming," *Aerospace Science and Technology*, vol. 50, pp. 149 – 160, 2016.
- [37] M. T. Hagan, H. B. Demuth, and O. D. Jes˜aos, "An introduction to the use of neural networks in control systems," *International Journal of Robust and Nonlinear Control*, vol. 12, no. 11, pp. 959–985, 2002.
- [38] O. Egeland and J. M. Godhavn, "Passivity-based adaptive attitude control of a rigid spacecraft," *IEEE Transactions on Automatic Control*, vol. 39, no. 4, pp. 842–846, Apr 1994.
- [39] Q. L. Zhou, Y. Zhang, C. A. Rabbath, and D. Theilliol, "Design of feedback linearization control and reconfigurable control allocation with application to a quadrotor uav," in *2010 Conference on Control and Fault-Tolerant Systems (SysTol)*, Oct 2010, pp. 371–376.
- [40] Q. Lu, Q. Han, B. Zhang, D. Liu, and S. Liu, "Cooperative control of mobile sensor networks for environmental monitoring: An event-triggered finite-time control scheme," *IEEE Transactions on Cybernetics*, vol. 47, no. 12, pp. 4134–4147, 2017.
- [41] R. Olfati-Saber and R. M. Murray, "Distributed structural stabilization and tracking for formations of dynamic multiagents," *Proc. IEEE Conf. Decision and Control*, pp. 209–215, 2002.

- [42] R. T. Jonathan, J. Lawton, R. W. Beard, and B. J. Young, "A decentralized approach to formation maneuvers," *IEEE Trans. on Robotics and Automation*, vol. 19, pp. 933–941, 2003.
- [43] R. W. Beard, J. Lawton, and F. Y. Hadaegh, "A coordination architecture for spacecraft formation control," *IEEE Trans. on Control Systems Technology*, vol. 9, no. 6, pp. 777–790, 2001.
- [44] R. Xu and U. Ozguner, "Sliding mode control of a class of underactuated systems," *Automatica*, vol. 44, no. 1, pp. 233 – 241, 2008.
- [45] S. Bertrand, N. GuÃ c nard, T. Hamel, H. Piet-Lahanier, and L. Eck, "A hierarchical controller for miniature vtol uavs: Design and stability analysis using singular perturbation theory," *Control Engineering Practice*, vol. 19, no. 10, pp. 1099 – 1108, 2011.
- [46] S. P. Bhat and D. S. Bernstein, "A topological obstruction to continuous global stabilization of rotational motion and the unwinding phenomenon," *Systems & Control Letters*, vol. 39, no. 1, pp. 63 – 70, 2000.
- [47] S. Zhao, W. Dong, and J. A. Farrell, "Quaternion-based trajectory tracking control of vtoluavs using command filtered backstepping," in *2013 American Control Conference*, June 2013, pp. 1018–1023.
- [48] V. Roldao, R. Cunha, D. Cabecinhas, C. Silvestre, and P. Oliveira, "A leader-following trajectory generator with application to quadrotor formation flight," *Robotics and Autonomous Systems*, vol. 62, no. 10, pp. 1597 – 1609, 2014.
- [49] W. Dong, J. A. Farrell, M. M. Polycarpou, V. Djapic, and M. Sharma, "Command filtered adaptive backstepping," *IEEE Transactions on Control Systems Technology*, vol. 20, no. 3, pp. 566–580, May 2012.

- [50] W. Jasim and D. Gu, "Robust team formation control for quadrotors," *IEEE Transactions on Control Systems Technology*, vol. 26, no. 4, pp. 1516–1523, 2018.
- [51] W. Ren and R. W. Beard, "Formation feedback control for multiple spacecraft via virtual structures," *IEE Proceedings - Control Theory and Applications*, vol. 151, no. 3, pp. 357–368, 2004.
- [52] X. Liu, J. Cao, W. Yu, and Q. Song, "Nonsmooth finite-time synchronization of switched coupled neural networks," *IEEE Transactions on Cybernetics*, vol. 46, no. 10, pp. 2360–2371, 2016.
- [53] X. Wang, S. Li, and P. Shi, "Distributed finite-time containment control for double-integrator multiagent systems," *IEEE Transactions on Cybernetics*, vol. 44, no. 9, pp. 1518–1528, 2014.
- [54] X. Wang, V. Yadav, and S. N. Balakrishnan, "Cooperative uav formation flying with obstacle/collision avoidance," *IEEE Transactions on Control Systems Technology*, vol. 15, no. 4, pp. 672–679, 2007.
- [55] Y. Cao, W. Ren, and Z. Meng, "Decentralized finite-time sliding mode estimators and their applications in decentralized finite-time formation tracking," *Systems & Control Letters*, vol. 59, no. 9, pp. 522–529, 2010.
- [56] Y. Zou, "Nonlinear robust adaptive hierarchical sliding mode control approach for quadrotors," *International Journal of Robust and Nonlinear Control*, vol. 27, no. 6, pp. 925–941, 2017.
- [57] Y. Zou, "Trajectory tracking controller for quadrotors without velocity and angular velocity measurements," *IET Control Theory Applications*, vol. 11, no. 1, pp. 101–109, 2017.

- [58] Z. Chen and J. Huang, “Attitude tracking and disturbance rejection of rigid spacecraft by adaptive control,” *IEEE Transactions on Automatic Control*, vol. 54, no. 3, pp. 600–605, 2009.
- [59] Z. Zuo and C. Wang, “Adaptive trajectory tracking control of output constrained multi-rotors systems,” *IET Control Theory Applications*, vol. 8, no. 13, pp. 1163–1174, September 2014.
- [60] Z. Zuo, “Adaptive trajectory tracking control of a quadrotor unmanned aircraft,” in *Proceedings of the 30th Chinese Control Conference*, July 2011, pp. 2435–2439.

## BIOGRAPHICAL SKETCH

Miguel Garcia began his M.S.E in Electrical Engineering at The University of Texas Rio Grande Valley in August 2021 after graduating with his B.S.E.E from the University of Texas Rio Grande Valley back in May of 2021, located in Edinburg, Texas. Throughout his graduate level education, Miguel worked as a graduate research assistant under the supervision of Dr. Wenjie Dong that was supported by the National Science Foundation where the focus of research was on feedback control methods and tracking control systems. Throughout his tenure Miguel also worked full-time as an electrical engineer for a growing, innovating company that focused on automation control. Miguel earned his Masters of Science in Engineering from the University of Texas Rio Grande Valley in May 2023. Graduating with his M.S.E in Electrical Engineering, Miguel hoped to join The University of Texas Rio Grande Valley as a lecturer to be able to share his knowledge with students wanting to follow the same path and to encourage more students to pursue a master degree. Miguel plans on going back to school to earn a Ph.D in electrical engineering however he would like to reward himself with a break to spend time with his loving wife and child.

To contact him for any information, please reach out to [garcia1754@gmail.com](mailto:garcia1754@gmail.com).